UNIVERSITY OF CALIFORNIA SAN DIEGO

Soil Behavior of High Aspect Ratio Pesticide Carriers

A thesis submitted in partial satisfaction of the requirements
for the degree Master of Science

in

NanoEngineering

by

Udhaya Pooranam Venkateswaran

Committee in charge:

Professor Nicole Steinmetz, Chair
Professor Zeinab Jahed Motlagh
Professor Jonathan Pokorski

2022

Soil Behavior of High Aspect Ratio Pesticide Carriers

The thesis of Udhaya Pooranam Venkateswaran is approved, and it is acceptable in quality and form for publication on microfilm and electronically.

University of California San Diego

2022

Table of Contents

List of Abbreviations

PEG : Polyethylene glycol

TMV : Tobacco Mosaic Virus

TMV-Lys : Tobacco Mosaic Virus with Lysine corona

TMGMV : Tobacco Mild Green Mosaic Virus

TMGMV-PEG2K : linear 2 kDa PEG conjugated TMGMV

TMGMV-PEG5K : linear 5 kDa PEG conjugated TMGMV

TMGMV-PEG5K4A: 4-arm 5 kDa PEG conjugated TMGMV

TMV-PEG2K : linear 2 kDa PEG conjugated TMV-Lys

TMV-PEG5K : linear 5 kDa PEG conjugated TMV-Lys

TMV-PEG5KB : bivalent 5 kDa PEG conjugated TMV-Lys

List of Symbols

Void Fraction = φ

Void Volume = V_{void}

Density of Soil = ρ

Max. Packing Density = ρ_{max}

Zeta Potential = ζ

Relative Mobility = μ

List of Tables

List of Figures

Acknowledgments

I would like to thank Professor Nicole Steinmetz for providing me with the opportunity to be a part of her research group and for her tremendous support and guidance throughout my journey. Her mentorship and timely pieces of advice have made this project what it is today.

Secondly, I would like to offer my sincerest gratitude to my mentor Adam Caparco, Ph.D., for deciding to spend his invaluable time to guide me throughout my journey. Without him, I would have never been able to finish the project, much less on time. I would never be able to thank him enough for choosing me to be his first student at UCSD and for helping me with the smallest of tasks and the most trivial questions.

Special thanks to Ivonne González-Gamboa, Ph.D., for sharing her technical expertise, and for always being the kindest person in the lab. I would also like to thank Justin McCaskill and Sabrina Chang for all the help they did throughout my thesis.

I would like to thank my fellow lab members Reca Cabellaro, Bryan Duoto, and Jorge Leganes Bayon without whom this project would have taken much longer to complete, and I also would like to thank the whole of Steinmetz Lab for their tremendous support, positive criticism, and encouragement throughout.

I would like to thank my family and friends in India and a very special thanks to my friends in San Diego who were the biggest pillars of support throughout my Master's journey.

This work was funded through research grant NIFA-2020-67021-31255.

Abstract of the Thesis

Soil Behavior of High Aspect Ratio Pesticide Carriers

by

Udhaya Pooranam Venkateswaran

Master of Science in NanoEngineering

University of California San Diego, 2022

Professor Nicole Steinmetz (Chair)

Pesticide usage in an abusive manner in agriculture causes health problems to society, disease and contamination of livestock, development of pesticide-resistant microorganisms in the soil, and poisoning of water bodies due to leaching. Overuse of pesticides is a critical issue that concerns the health of the environment, plants, animals, and humans – and therefore there is a need for next-generation nanotechnology-driven solutions. Plant virus nanoparticles (VNPs) provide a platform that can be used as nanocarriers for the targeted delivery of pesticides in small and controlled doses while being robust, biodegradable, and versatile. While plant viruses are pathogens to plants – they also evolved to interact with plants and soil because they are

plant pathogens. The idea here is to repurpose the biology of plant viruses for precision farming. In previous work, it was shown that plant viruses from tobacco mild green mosaic virus (TMGMV) have good soil mobility. In this work, I addressed structure-function questions: (i) how the soil properties impact plant virus carrier mobility and (ii) how the plant virus surface chemistry impacts its soil mobility – again as a function of soil property. I tested soil mobility in four soil types and assessed soil mobility of native vs. PEGylated plant viral carriers. A combination of chemical synthesis, nanoparticle characterization, and soil mobility assays was used. Data indicate that the soil mobility of the VNPs was greatly enhanced by modifying their surface.

Chapter 1 Introduction:

1.1 Introduction to precision farming:

Due to the exponentially growing population, the demand for food has thus increased consequently. Be it for animal or human consumption, basic food security is a concern with limited resources and increased demand for food crops [1]. Due to this surge in demand, pesticides, fertilizers and anti-weed control measures have been extensively used in the current agricultural setup to achieve two main objectives: Increased yield and control of soil condition for future use [2].

The statistics for the year 2022 have shown that over 345 million people do not have economic access to food and are on the verge of acute food insecurity as per the report from The World Food Program (WFP USA) [1]. These statistics and the trend in food insecurity have shown that with limited resources, it is essential to identify and implement core changes in how we, as a society, deploy agricultural practices and use scientific knowledge and techniques in enhancing yield while not causing catastrophic damage to the ecosystem.

In order to implement these changes, agronomy must be employed. Agronomy is the management of soil and crop production and has seen significant scientific interest over the years due to climate change, insufficient crop yields, and the demand for food crops. The need to sustainably access and use natural resources while also meeting the demands in a more eco-friendly way has also gained research attention from around the world [3, 4]. Soil degradation, water scarcity, and reduced fertility of soil are all factors that force farmers to engage in the practice of industrial farming. Industrial farming was introduced shortly after World War 2 to constantly maintain and increase the production of food crops to meet worldwide demand. Slowly, the agricultural systems also started using fast-yield crops and preferred fast

crop rotations to further support global economic demand for food [3]. This led the agricultural ecosystems to become severely distressed and caused irreversible damage to the soil, the crops, the groundwater systems, and nearby water bodies as well. This was done with the excessive use of pesticides, and other yield-enhancing agrochemicals to boost the production of essential crops while the microbiology of the soil was left unattended and mismanaged.

The overuse of pesticides and herbicides such as glyphosate also leads to short-term and long-term effects on humans due to the residual pesticides on food crops and also causes tissue and organ damage in the human body [5]. Many pesticides are often applied in their powder form and tend to be inhaled or ingested by the farmers which causes direct immunological complications and fatal diseases such as respiratory diseases, cancer, and dermatological diseases [6]. There are several reports over the years that have shown the adverse effects of the bioaccumulation of pesticides as they were detected in vegetables [7], and even in milk [8]. Resources, such as water and the area of fertile soil, continue to decline whereas the demand on the other hand keeps rising and as per the report from the United Nations Department of Economic and Social Affairs (UN DESA), the population on our planet is projected to reach 9.7 billion by 2050 and to 10.4 billion by 2100.

Another key concern is soil degradation, which is the primary cause of lower crop yields. When crops are rotated too fast with excessive use of pesticides and without adequate time for the organic matter in the soil to develop, along with severe climatic conditions caused by global warming, the soil quality deteriorates resulting in poor economic returns for the farmers. However, with reduced use of pesticides, the yield and the food quality declines rapidly as a consequence. For example, the Great Irish Famine, due to which over a million Europeans faced acute food shortage and starvation, was caused by the destruction of potato crops by a plant disease called late blight. Another recent example is the devastation of maize fields in

Kenya and eastern Africa in 2011 by maize lethal necrosis (MLN). It has also been reported that plant viruses result in an astonishing 30 billion USD loss annually around the world [9] with incidences of plant viruses being responsible for 100% yield losses resulting in great economic impacts [10]. Hence a new method of delivery of these pesticides is a much-needed solution.

The excessive application of pesticides leads to pesticide-resistant microorganisms, wherein the essential and infectious microorganisms, such as bacteria, in the soil that would generally die with a small quantity of pesticide start to resist and demand higher doses of pesticides to be applied to be subdued. Microbial resistance to pesticides also leads to genetic mutation of pesticide-sensitive microorganisms to become resistant and creates a strain on microorganisms that are not affected by the use of pesticides [11].

Another major issue with the abusive use of pesticides is the leaching of pesticides into water ecosystems [12]. This leads to water-borne microorganisms as well as plants and water animals being severely affected and exposed to toxins. Altering the optimal aquatic conditions also affects the consumption of freshwater sources and requires more stages in purification before water can be used for agriculture and farming practices. Eutrophication of freshwater as well as its negative impact in the coastal zones are a major concern that accompanies the abusive and inefficient use of pesticides on food and production crops according to a report published by the United Nations Environment Programme (UNEP) [13]. This is especially more evident in arid regions around the world where the availability of water is already limited and hence adverse effects of the abuse of pesticides further decrease and render the water available for consumption unusable. All of these issues leave us with the question of what can be done to address the pressing issue of the usage of pesticides while preserving and enhancing the soil fertility and sustainability of the agricultural ecosystem while containing and improving the agri-supply chain and stakeholder engagement. The obvious answer is the

reduced use of pesticides; smaller doses at a lower frequency. A need for more targeted pesticide delivery with the use of materials that have improved soil mobility and also do not attribute the prevailing problem of bioaccumulation of pesticides in soil and aquatic sources. Novel methods are required to ensure the biocompatibility and natural decomposition of these synthetic pesticides by ensuring a lower duration of retention in soil and aquatic habitats. Such next-generation pesticides also need to be scalable, effective, and non-toxic to both humans and other non-target organisms. An alternative method of solving such issues is through Genetic Engineering. GE is a process where organisms can be modified in a laboratory to increase the desired trait of the organism. Several successful attempts in the field of agriculture have been reported and one such example is the invention of the Golden Rice by Ingo Potrykus and Peter Beyer who sought to address the issue of Vitamin A deficiency causing childhood blindness Golden rice is a generic name given to genetically modified rice that has an enriched amount of provitamin A [14]. The use of genetically engineered seeds to withstand the abuse of pesticides, herbicides, and insecticides is prevalent now, with more than 90% of the current high-yield crops such as corn and soybean being genetically modified organisms (GMOs) [15]. Such GMOs can withstand harsh and direct application of pesticides such as glyphosates and are also immune to almost all common plant viruses.

1.2 Nanoparticles in agriculture:

As the world moves ahead with dwindling resources, it is important to realize the importance and advantages of using nanotechnology as a platform to improve the materials usage properties as well as conserve the number of materials used. Nanotechnology refers to the use of materials at the nanoscale to combat challenges such as drug delivery in biomedical applications and treatments, pesticide delivery in agricultural applications, and a plethora of fields in which it holds the potential to enhance the outputs. Next-generation pesticides and their

regulated and efficient usage should then grow to greater heights with the help of leveraging the use of nanotechnology in agriculture practices [16]. Nanotechnology can help us create next-generation pesticides. Nanosuspension and nanocolloids are nanoparticles of pesticides, herbicides, and insecticides suspended in a solution to be used in the agricultural framework and can be classified into two fundamental categories namely (1) organic molecular structures loaded with active ingredients (AI) and (2) inorganic nanoscale AI [17]. The core idea behind the use of nanoengineering principles in pesticide and fertilizer usage has been to drastically reduce the amount of material used on the soil and to target the intake of these nanoparticles (NP) by the plant. Targeted and non-targeted pesticide delivery using synthetic [18], polymeric and biodegradable [19], and plant viral nanoparticles [20] has been a field of growth in the past decade. Using nanoformulations for pesticides also enhances the bioavailability of AI to plants and crops, and improves the water solubility of pesticides that are generally insoluble in water [21].

However, even when using nanopesticides, they come with several risks such as bioaccumulation, toxicity to non-target organisms, and transportation risks [17]. Hence, the need for pesticide carriers comes into play that keeps much of these risks to a minimum. The pesticide carriers must be biocompatible to not cause further pollution of soil. Along with this, the slow and controlled release of AI that are loaded onto the nanocarriers is needed to effectively counter the issue of overuse of pesticides and insecticides. Biocompatibility is an important factor when using nanopesticides. It ensures that more toxicity or pollution of the soil is not prevalent after switching from bulk pesticides to nanopesticides.

1.3 Plant virus nanoparticles (VNPs):

In light of issues such as high energy-intensive manufacturing, multi-stage chemical synthesis, laborious processes, and toxic by-products as a result of conventional nanomanufacturing of synthetic nanomolecules, the increased demand for more robust, sustainable, and “smart material” leads us to functionalize natural biomolecules [22]. One such material that has recently gained popularity for its biocompatibility and versatility is plant viruses. Although viruses are generally seen as pathogens that cause harm, plant viruses have a different host range than those of vertebrate viruses and have been reported to be safe for human exposure [23]. These plant virus nanoparticles (VNPs) are ordered structures of protein materials that targets and infects plants – naturally evolved to package their genome, but through synthetic biology and engineering, the natural cargo can be replaced with AI and delivered to target locations. Plant viruses being pathogens to plants have evolved to interact with plants and the soil – these properties can be exploited for agricultural nanotechnology. There are over 900 plant viruses that are now recognized by the International Committee on Taxonomy of Viruses (ICTV) [24]. Virus like nanoparticles (VLP) are materials that resemble the native viruses however repurposed for medical, veterinary, or agricultural applications [25]. Platforms such as inactivated VNPs from tobacco mild green mosaic virus (TMGMV) [26] have been developed and tested in soil-borne delivery of pesticides and other cargo to the roots and fight nematodes present in the soil [28].

Since there are a variety of plant viruses that differentiate by size, protein structure, surface properties, and other biochemical properties, we can use the nanotechnological arsenal to repurpose and tailor them to meet our goal of pesticide delivery. Tobacco mosaic virus (TMV) which is the first virus to have been described [29] has been repurposed for drug delivery

amongst many other applications in nanomedicine [30], but also in materials science [31]. VNPs such as cowpea mosaic virus (CPMV) [32], cowpea chlorotic mottle virus (CCMV) [33], and potato virus x (PVX) [34] have also gained research attention in nanomedicine research and are being engineered for drug delivery, vaccines, etc. Several of these plant viruses also hold the potential to be spatially transformed and biologically redesigned. For example, native TMV (300 x 18 nm) which has a rod-like structure has been reported to be able to self-assemble into bidirectional encapsidation and form complex branched nano objects [35] through tailored RNA and modified coat protein (CP) methods. These complex protein structures can also be modified through external conditions such as heat and thermal transformation. An example of this is the two-step thermal transformation of the rigid helical rod-like TMV into a Spherical Nanoparticle (SNP) at 94°C [36]. This results in key noticeable improvements such as increased robustness as the size of the SNPs remained only dependent on the concentration of the TMV used. The resulting SNPs can be size-controlled by adjusting the starting protein concentration. It is also reported that the TMV-to-SNP transition allowed the SNPs to become more stable as the size of the SNPs remained unchanged even after storing at 4 for close to 6 months which presents an interesting venue in terms of storage and transportation of these particles. During the transformation process, the SNP is reported to be consisting of thermally denatured CP and free of the viral RNA strand which is confirmed by the study. Another example of the thermal transition of virions into SNPs is reported using the flexuous filaments of the PVX which resulted in a more dense arrangement of the CPs compared to the native, flexuous counterpart [37]. It is also reported that the thermal transition occurred at a lower temperature than TMV and that the size of the SNPs did not depend entirely on the initial concentration of PVX used for the transformation, however, it is noted that the thermal transformation resulted in RNA-free SNPs. These examples confirm the customizability of these VNPs and help to realize the potential of VNPs as a platform to create tailor-made nanopesticide carriers.

In addition to their physical structural changes, they can also be “decorated” in known patterns and target locations on or on the surface through physicochemical processes such as bioconjugation reactions. The bioconjugation reaction is a process of forming a covalent bond between two or more biomolecules with polymers or other materials. An example is the azide-alkyne click reaction using the TMGMV platform [38]. Using these reactions and methods, we can greatly alter and tailor the properties of the VNPs to suit our desired applications for AI delivery while retaining important conditions such as biocompatibility.

1.4 Tobamoviruses and precision farming:

In my work, I specifically focused on the tobamovirus TMGMV as well as TMV-Lys – the nucleoprotein structures measure 300 x 18 nm with a 4 nm-wide hollow canal constructed with over 2,000 identical coat proteins surrounding one molecule of a single-strand RNA [39]. TMGMV affects the pepper plants causing defoliation, systemic necrosis, and chlorotic mosaic hence reducing the quality and yield of pepper harvest [40]. In contrast, TMV has a broad host range [41]. TMGMV is readily available commercially, and it has been approved by the United States Environmental Protection Agency (US EPA) for bioherbicidal and agricultural applications [42].

TMV, which is also a member of the tobamovirus species can have multiple genetic variants and one such variant is the TMV-Lys with a Threonine-to-Lysine substitution with the exposed surface of TMV-Lys displaying a corona of lysine side chains [43]. TMV and TMV-lys are both invaluable when it comes to surface availability for bioconjugation and have proven to be more reproducible as well. TMV and TMGMV are from the same family of viruses and thus have similar properties and structures.

Agricultural application of nanopesticides often poses a multitude of variables to understand the performance of efficacy, of which soil mobility of these particles plays a key role in understanding the interactions between nanopesticides and the soil molecules. A study on the soil mobility of synthetic and virus-based pesticides was performed in laboratory conditions that mimicked real-life agricultural conditions and a dye molecule (Cy5) was used as the cargo and was either conjugated or encapsulated with the nanoparticles. TMGMV was reported to be the best-performing carrier that was able to reach a depth of 30 cm irrespective of the method of cargo loading. Thus the study revealed that the soil mobility of TMGMV was greater than other VNPs and also synthetic carrier molecules such as mesoporous silica and PLGA [44]. This study also showed that the analysis of the amount of Cy5 dye that was encapsulated decreased with the soil depth indicating that it was released over time as the carrier molecule was eluted through the soil sample.

Further, a study was conducted to show proof-of-concept of AI delivery using TMGMV: here, TMGMV was loaded with the anthelmintic drug crystal violet (CV) and delivery was carried out to target *Caenorhabditis elegans* (*C. elegans*) nematodes [28]. The study revealed the enhanced soil mobility of the TMGMV loaded with CV compared to free CV and displayed the efficacy as the bioavailability of the pesticide drug is reported to be higher when using the TMGMV than when using free CV. Such studies show the importance to understand and study the behavior of these highly modifiable VNPs.

Chapter 2 Aims of this thesis:

Previous soil mobility studies using plant viruses such as TMGMV [44] were performed only using a single type of soil and only considered native TMGMV. However, in agricultural practices around the world, a multitude of different soil types are used for different crops due to geological conditions. Therefore, the results using a single type of soil could not be used to determine the performance of the VNPs in different soils as we know that the soil chemical composition, texture, organic matter, and other properties vary between each soil. In addition, the interactions between the soil molecules and the surface of the VNPs are hypothesized to have an impact on soil mobility. This gap in the knowledge pertaining to the performance of VNPs in different soil types must be addressed.

Toward this goal, in this work, I studied TMGMV and TMV-Lys as model systems, and native and PEGylated formulations were studied. Additionally, I also used PVX and PhMV to differentiate the soil behavior between high-aspect ratio rod-like virus, icosahedral virus, and flexuous virus types. In addition to addressing structure-function studies, I also focused on method development for the analysis of VNPs in soil columns. I focused on two objectives in this study:

1) Develop a BCA protein assay for soil mobility application

2) Asses the effects of surface modification of VNP and soil type on soil mobility

For PEGylation, linear vs. bivalent PEG with a molecular weight of 2 kDa vs. 5 kDa was compared and I used 4 different soil types (MTS, Veggie, Potting, and 50/50) to understand the interactions that exist between the nanoparticles and the soil molecules. The BCA protein assay was established as an alternative to the SDS-PAGE method to analyze the soil content.

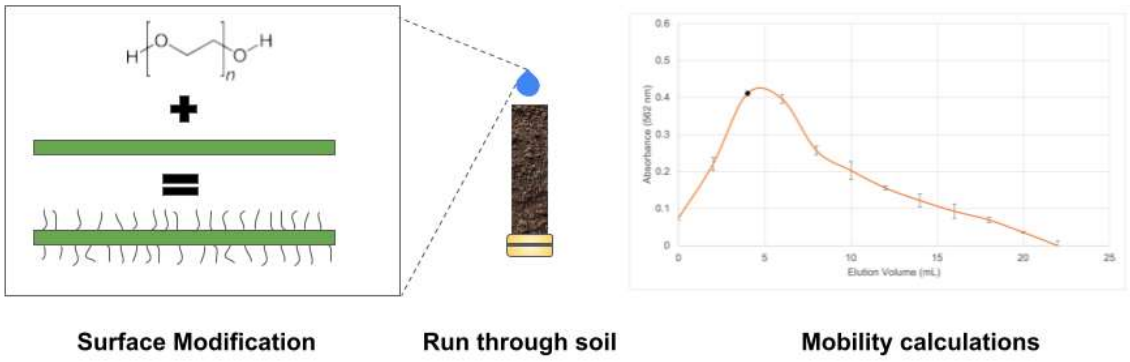

Figure 2.1: Schematic representation of the methodology for VNP soil mobility measurements

Chapter 3 Materials and Methods:

3.1 Materials:

Unless otherwise specified, materials were provided by Fisher Scientific (Waltham, MA, USA).

3.2 Preparation of viruses and viral nanoparticles purification:

The TMGMV used in this study was procured from BioProdex (Gainesville, FL, USA) and stored at 20°C until use. The obtained solution was thawed at 4°C overnight and then dialyzed against potassium phosphate buffer (KP; 10 mM, pH 7.2) for 24 hours at 4°C using 12–14 kDa dialysis tubing (Fisher Scientific S432700; Waltham, MA, USA). The buffer solution was replaced, and the dialysis continued for an additional 48 hours. The solution was then centrifuged at 10,000×*g* for 20 min (Beckman Coulter Allegra or Avanti centrifuges). The supernatant was collected and ultracentrifuged at 12000x*g* for 2.5 hours at 4°C (Beckman Coulter OptimaL-90k Ultracentrifuge with 50.2 Ti rotor; Brea, CA, USA). The pellet was resuspended under rotational mixing overnight at 4°C in KP buffer. The sample concentration was then confirmed using a Nanodrop 2000 (Thermo Scientific; Waltham, MA, USA); the concentration was adjusted to 10 mg mL^{-1} in 10 mM KP before storing at 4°C (for TMGMV CP, ε_{260} = 3 mL mg^{-1} cm^{-1}) [38].

The TMV-Lys, Cy5-TMV-Lys, and PEG-TMV-Lys were characterized and provided by Reca Caballero (Steinmetz Lab, UCSD, CA, USA). The PVX was characterized and provided by Bryan Duoto (Steinmetz Lab, UCSD, CA, USA). The PhMV was characterized and provided by

Jorge Leganes Bayon (Steinmetz Lab, UCSD, CA, USA). The TMV-Lys was isolated and purified from systemically infected *Nicotiana benthamiana* [37] and to confirm the presence of lysine residues, 0.5 mg TMVLys nanoparticles were reacted with 4,000 molar equivalents of Sulfo-Cyanine5 NHS ester (Lumiprobe). In specific for the PEG conjugation, 2.5 mg of TMV-Lys nanoparticles were reacted with linear or branched PEGs (2 kDa linear, 5 kDa linear, 5 kDa bivalent) at 40:1 CP and 20:1 CP molar excess, respectively, in potassium phosphate buffer (KP; 10 mM, pH 8). The reactions were carried out in 10% (v/v) DMSO in 0.01 M potassium phosphate buffer (pH 8) and agitated overnight at room temperature in the dark. The functionalized nanoparticles were then purified via ultracentrifugation at 10000x*g* (Beckman Optima MAX-XP with TLA-55 rotor) over a 30% (v/v) sucrose cushion for 1 hour. The supernatant was removed, and the pellet was resuspended under rotational mixing at 4°C overnight before further characterization.

United States Department of Agriculture permits (P526P-21-02414) were obtained for any work with plant viruses.

3.3 Preparation of diazonium salt from 4-ethynylaniline:

In a 5 mL tube, 298 mg of 4-ethynylaniline was dissolved in 2 mL methanol. In a 50 mL tube, 1.09 *g* *p*-toluene sulfonic acid was dissolved in 20 mL DI H_2O. Both solutions were placed at 20°C for 10 minutes to precool. A solution of 1.5 mL of 3 M sodium nitrite (258 mg in 1.5 mL DI H_2O) was prepared and placed at 20°C for 5 minutes to precool. A 50 mL beaker was submerged in ice/water slurry on a stir plate. The solutions were removed from the freezer. A stir bar was added to the 20 mL of precooled acid in the submerged beaker. Once mixed, the methanol solution was added. The solution turned opaque and beige in color. The nitrite solution was gradually dropped into the acid solution and the mixture gradually turned yellow and

eventually turned red after 30–60 minutes of reaction time. A sample of 1 mL of the diazonium slurry was collected and centrifuged for 2 minutes at 10,000×*g* to isolate diazonium salts. On the ice, the supernatant was removed and the diazonium salts were resuspended in 1 mL of precooled ethanol. The prepared diazonium salts were used immediately for tyrosine modification [38].

3.4 Coupling of diazonium to TMGMV:

A solution of 0.962 mL of 2 mg mL^{-1} TMGMV in 100 mM borate buffer (pH 8.5) was prepared and precooled on ice. The diazonium salt solution was added to the TMGMV solution at a volume of 0.080 mL. The solution was mixed by inversion and reacted on ice for 30 minutes. The solution was centrifuged at 10000x using the tabletop ultracentrifuge (Beckman Optima MAX-XP with TLA-55 rotor) for 1 hour with a sucrose cushion (30% v/v). The viral pellet was resuspended in 10 mM KP overnight at 4°C on a rotary shaker [38].

3.5 PEG conjugation of TMGMV:

To an ultracentrifugation tube (Beckman Coulter 357448, Indianapolis, IN, USA), 1 mg of TMGMV with diazonium was added. The reaction medium consisted of 1 mM copper sulfate, 2 mM aminoguanidine, 2 mM L-ascorbic acid, and 3.7 mM tris(benzyl triazolyl methyl)amine. The equivalences of the reactive PEG (2 kDa linear) per TMGMV coat protein were varied, and the volume of the KP buffer was adjusted for a final volume of 0.5 mL. PEGs were dissolved in DMSO before adding to the reaction mixture. The reaction was left to progress for 1 hour on ice. To the bottom of the same tube, a 0.2 mL sucrose cushion (30% w/v) was added, and the sample was then ultra-centrifuged at 10000x*g* for 1 hour at 4°C (Beckman Optima MAX-XP with

TLA-55 rotor). The supernatant was removed, and the pellet was resuspended using a 2-second sonication (QSonica Q500; QSonica, LLC, CT, USA) at 40% power on ice before further characterization [38].

3.6 Characterization of chemically labeled TMGMV and TMV nanoparticles:

SDS-PAGE: Denatured TMGMV or PEG conjugated TMGMV samples (20 µg) were loaded on a 12% NuPAGE gel (Life Technologies) and run in 1× MOPS Running Buffer (Life Technologies). Gel Code Blue stain (Life Technologies) was used to stain proteins and visualize them under white light.

Bands were analyzed using ImageJ software. ImageJ is a public domain software package (NIH, USA) that enables scientific image analysis. The band intensities of the molecular weight markers were analyzed by following the procedure outlined in a previous study for recombinant protein quantification [45].

SDS-PAGE was also used to analyze fractions collected from soil columns.

3.7 TEM imaging:

Samples were diluted to 0.05 mg mL^{-1} and absorbed onto carbon-coated TEM grids (Electron Microscopy Sciences). The grids were then washed three times with DI water. Then, grids were stained with 2% (w/v) uranyl acetate for 2 min for imaging. TEM was conducted using an FEI Tecnai F30 transmission electron microscope operated at 300 kV.

VNP size was analyzed using the ImageJ software package that allows image analysis. Using the TEM images of the surface-modified and native VNPs, particle lengths were determined manually by selecting the scale bar to calibrate the Measure Tool, following which straight lines were drawn on top of the particles individually. I report an average measurement (N=10) to obtain average particle size expressed as average particle length (nm) ± standard deviation (SD) and performed following the procedure outlined in [46].

3.8 Zeta Potential measurements:

Particle samples were diluted to 0.01 mg mL^{-1} in DI H_2O and 10 µL was loaded into the DTS1070 cuvette with the remaining volumes filled with DI H_2O. Zeta potentials were measured using the Zetasizer NanoZS (Malvern Panalytical; Westborough, MA, USA). Measurements were run in triplicates (N=3) and expressed as zeta potential (mV) ± standard deviation (SD).

3.9 Soil Mobility Assays:

Soil columns were made from 50 mL Falcon tubes with the bottom end cut. The bottom ends were covered with a 2.5" cheesecloth. The soil was prewet using a beaker with DI H_2O. The water-saturated soil was packed into the tube from the top using a spatula. Particles to be tested were added from the top following which water droplets were added to the soil columns from the top using a syringe pump at a constant flow rate of 5.0 mL min^{-1} and fractions were collected using 0.5 and 2 mL tubes for soil mobility analysis. Measurements were made in triplicates (N=3).

3.10 Bicinchoninic acid (BCA) Protein Assays:

Soil eluent was centrifuged for 15 seconds to remove sediments and the supernatant was collected. A 1:8 dilution of eluent was used in a BCA assay and the working reagent was made in the ratio of 1:9 according to the manufacturer's protocol (Thermo Fischer Scientific; Waltham, MA, USA). Samples were run in triplicates (N=3). Using a Tecan (Infinite 200Pro) plate reader, sample absorbance was measured at 562 nm wavelength and compared to a standard curve of bovine serum albumin.

3.11 Soil Analysis by Western Laboratories:

A comprehensive soil analysis was conducted for each soil in this study by Western Laboratories (Parma, Idaho, USA). The Magic Topsoil was provided by a local vendor, and the other soils were provided by SoCal Mulch (Menifee, CA, USA).

Chapter 4: Results and Discussion

4.1 VNP synthesis and characterization:

TMGMV and TMV were obtained and purified from infected leaf tissue. The integrity of the virus preparations was confirmed by size exclusion chromatography (Figure 4.1) and SDS-PAGE (Figure 4.2). In this work native and PEGylated TMGMV and TMV were used. For PEGylation surface engineered Lysine side chains on TMV were targeted and for TMGMV solvent-accessible Tyrosine side chains. First TMGMV modifications were performed Tyrosine residues were targeted using a Diazo-coupled reaction as described in the methodology section. Because the chemistry was low yielding (see data and discussion below), I also used PEGylated TMV. The advantage of TMV is that it offers a corona of solvent-exposed Lysine readily available for conjugation with NHS-activated esters. TMV modified with 2K linear and bivalent as well as 5K linear were obtained.

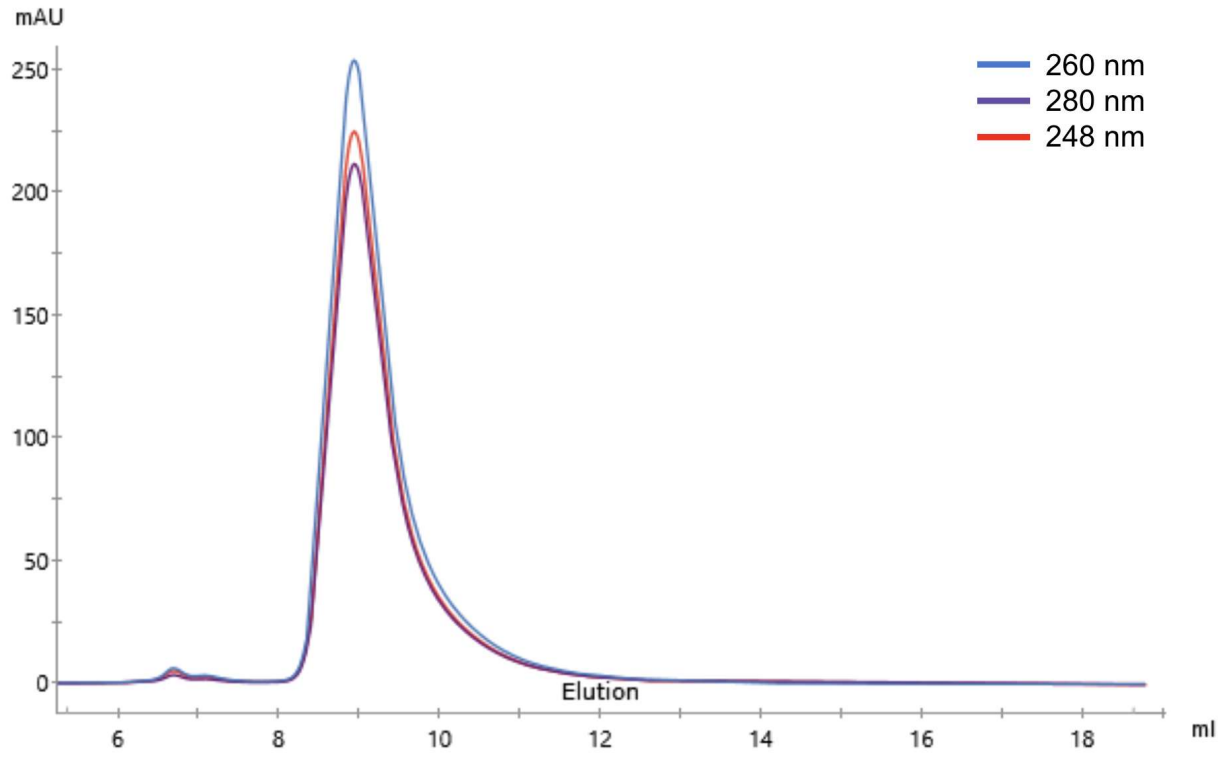

Figure 4.1: Size exclusion chromatography to analyze the purity of TMGMV

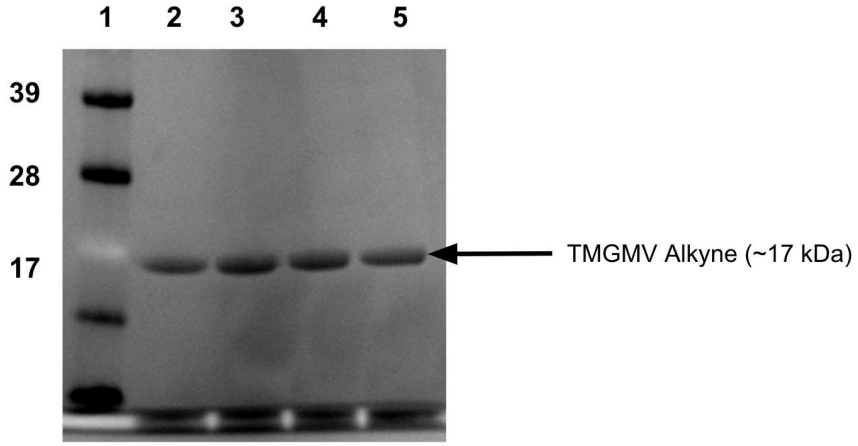

1: Ladder
2: native TMGMV (control)

3: TMGMV Alkyne (after diazonium coupling)
4: TMGMV Alkyne (after diazonium coupling)
5: TMGMV Alkyne (after diazonium coupling)

Figure 4.2: SDS-PAGE for native TMGMV before and after diazonium coupling

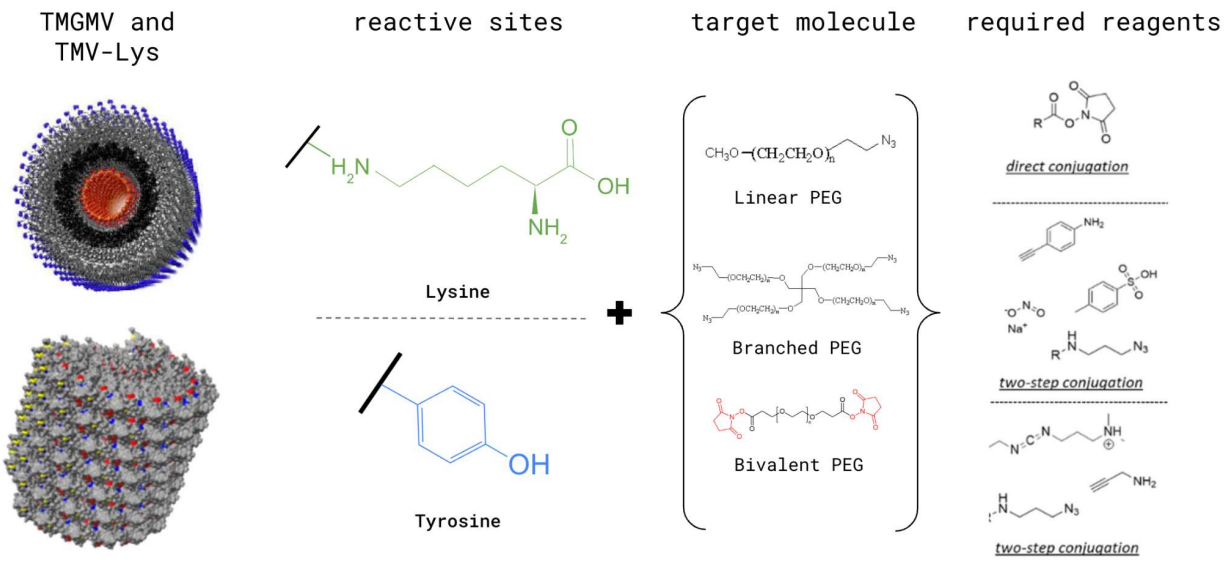

Figure 4.3: PEG conjugation strategy with lysine and tyrosine reactive sites on TMV and TMGMV respectively. Linear and branched PEG chains with molecular weights of 2 kDa vs. 5 kDa as well as bivalent PEG chains with a molecular weight of 5 kDa were used as target molecules to conjugate

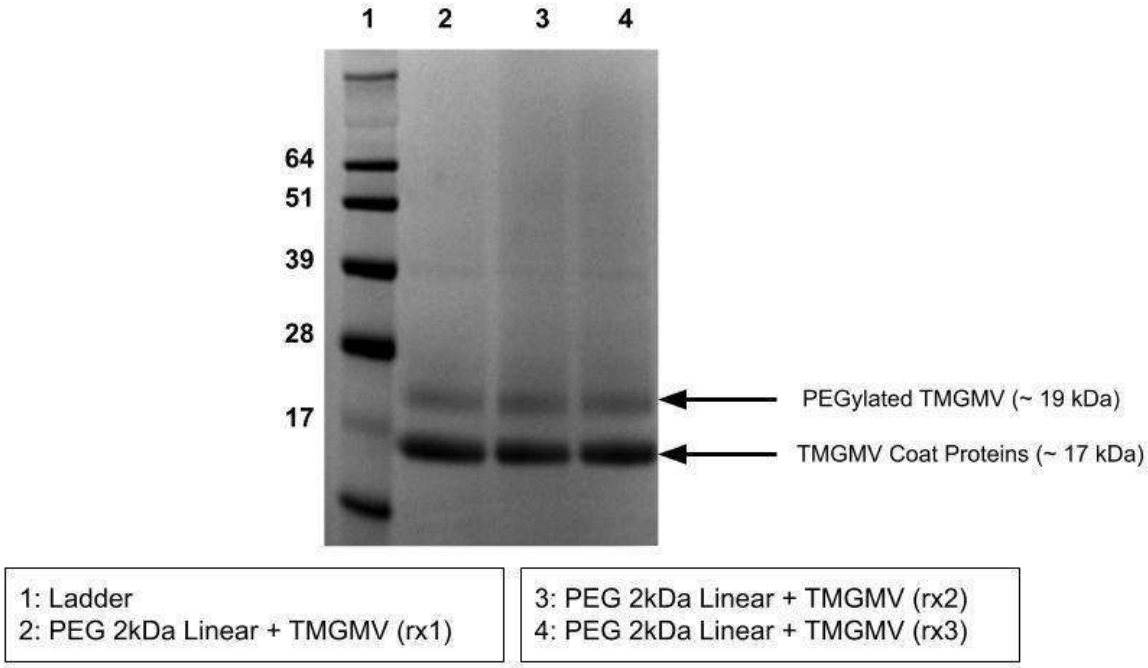

Figure 4.4: SDS-PAGE image of TMGMV-PEG2K after purification

Conjugation of PEG to TMGMV was confirmed by SDS-PAGE and the appearance of higher molecular weight bands (Fig 4.4). First, I analyzed native and azide-functionalized TMGMV on SDS-PAGE which showed the characteristic 17 kDa protein band; azide has a low molecular weight, and therefore a change in CP mobility is not observed (Figure 4.3). Native TMGMV coat protein (CP) has a molecular weight of 17 kDa; the addition of the PEG (MW 2 kDa) results in a 19 kDa CP-PEG band. ImageJ revealed that the average Degree of Labeling (DOL) was 27% ± 4%, i.e. how many PEG chains are attached. Previously small molecules (dyes and biotin) were conjugated to TMGMV yielding ~39% labeling [38]; my data is thus in good agreement – the slightly lower efficiency is explained by the high molecular weight of the PEG (2 kDa).

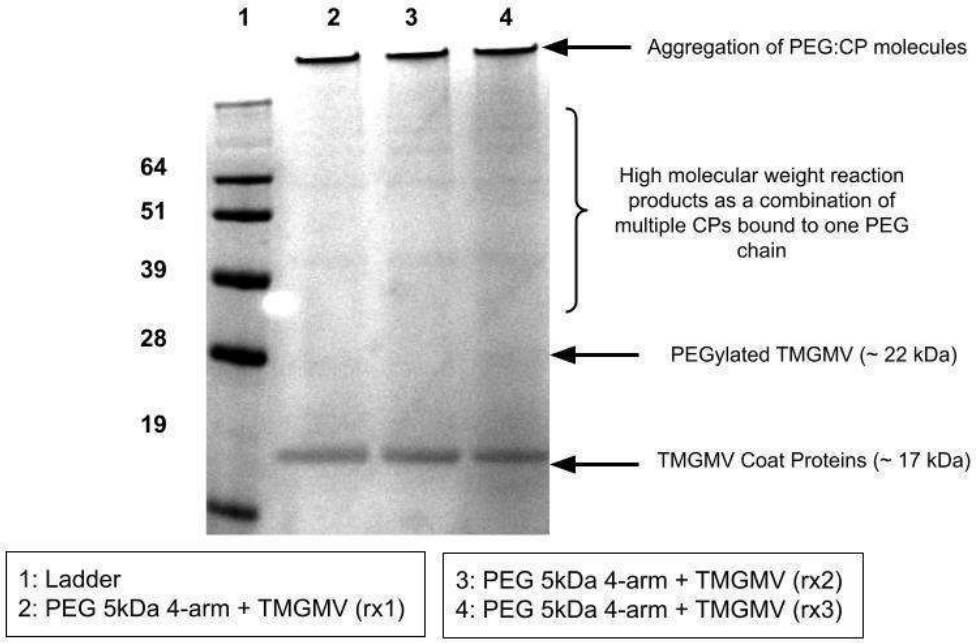

Figure 4.5: SDS-PAGE image of TMGMV-PEG5K4A after purification

However, when a branched PEG chain such as the 5 kDa 4-arm PEG chain is used in the bioconjugation reaction with TMGMV (Fig 4.5), I observed high molecular weight reaction products and aggregation of the VNPs. The aggregation was likely due to the micelle-like formation of the 4-arm PEG chain and due to intramolecular crosslinking [47]. This reaction did not produce uniform products with a defined molecular weight. Subsequent attempts to optimize the reaction at lower equivalences of PEG:TMGMV CP (1, 2, 5, and 10 PEG:CP) did not lead to defined reaction products. Thus, these VNPs were not considered for future soil mobility measurements.

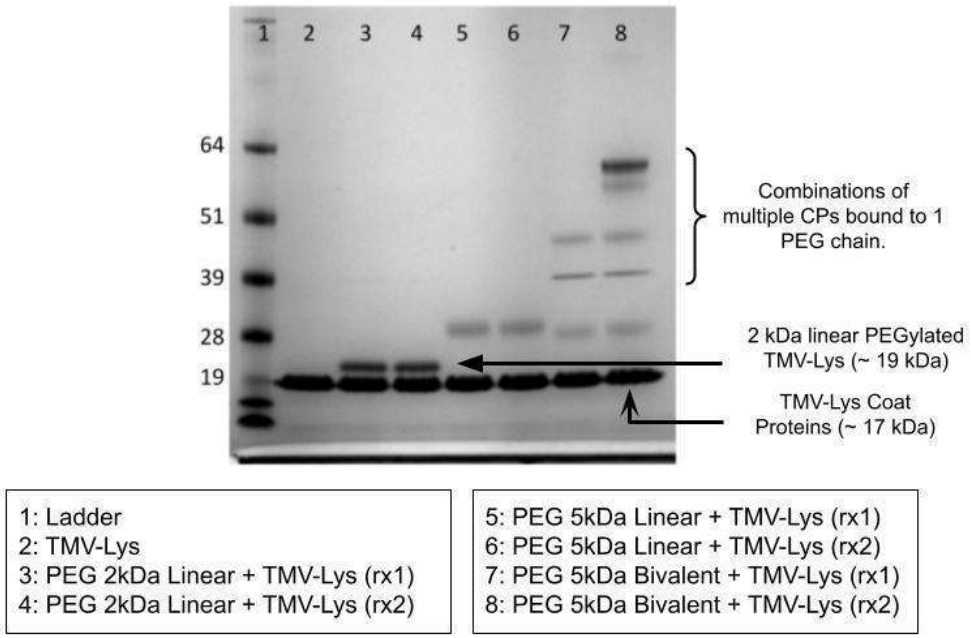

Figure 4.6: SDS-PAGE image of TMV-PEG2K, TMV-PEG5KB, TMV-PEG5K after purification

NHS-active esters were used and PEGylated TMV was purified by ultracentrifugation and then analyzed by SDS-PAGE, zeta potential measurements, and TEM analysis. SDS-PAGE confirmed successful PEG conjugation to TMV for each type of PEG, with different molecular weight distributions and conjugation efficiencies for each. ImageJ was used to analyze the gel for conjugation efficiency and was observed that the average DOL for the 2 kDa linear chain with TMV was 34%, the 5 kDa linear chain with TMV was 21% and the 5 kDa bivalent chain with TMV had the highest with a 42% average DOL. Fig 4.4 shows the TMV CP at 17 kDa and the PEGylated CP-PEG at 19 kDa Similar, TMV-PEG5K samples showed the characteristic CP band at 17 kDa and CP-PEG5K at 22 kDa (Fig. 4.6 lanes 5 and 6). For the bivalent TMV-PEG5K4A, the conjugation pattern is more complex: the CP at 17 kDa band as well as CP-PEG5K at 22 kDa, CP-PEG5K-CP at 39 kDa and higher order CP aggregates at 44 kDa and 54 kDa. Entangled CP-PEG conjugates also likely form dimers and trimers and are detected on SDS-PAGE.

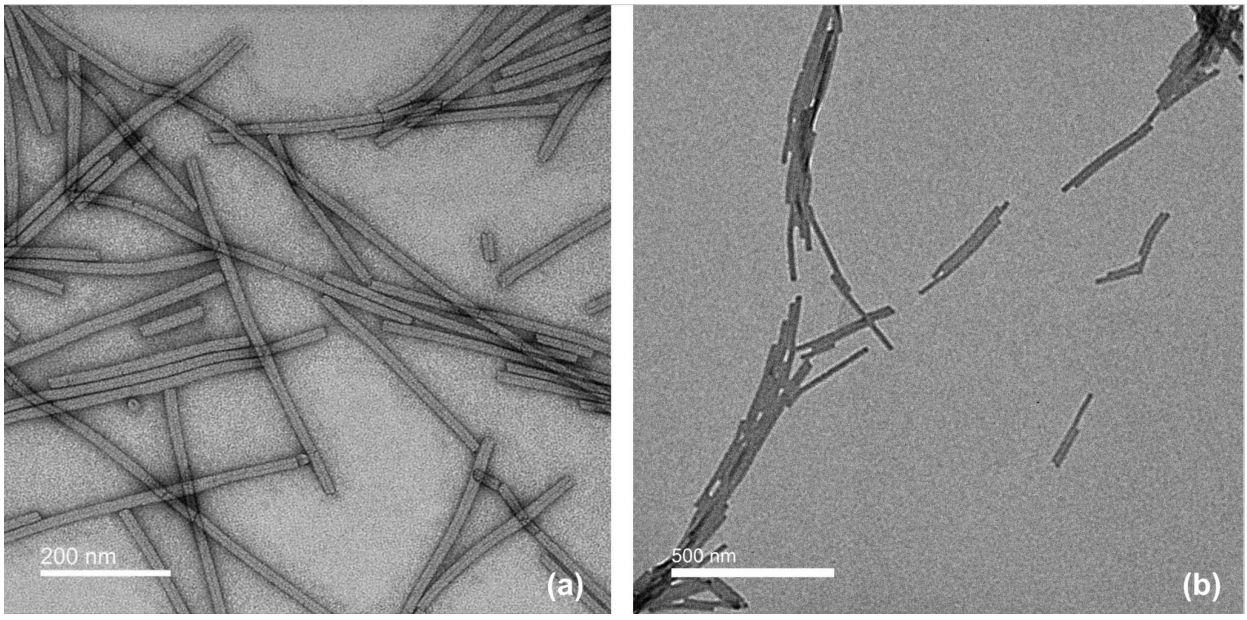

Figure 4.7: TEM of native TMGMV and TMV-Lys after purification

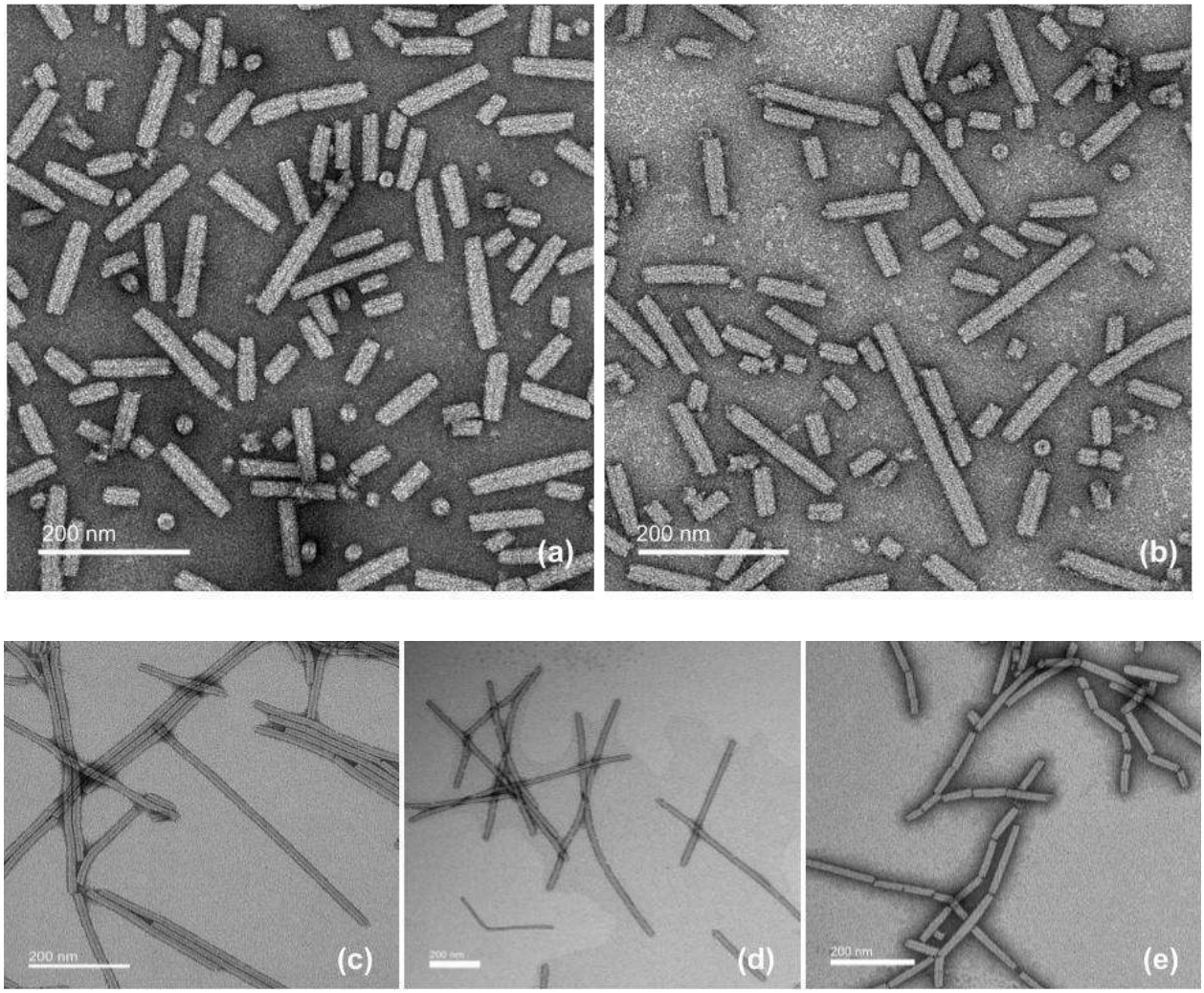

Figure 4.8: TEM of negatively stained (a) and (b) TMGMV-PEG2K

(c) TMV-PEG2K, (d) TMV-PEG5KB and (e) TMV-PEG5K

Fig 4.7 shows the TEM images of the native TMGMV and TMV showing the characteristic high aspect ratio nucleoprotein structures. Native TMV measures 300 x18 nm; in TEM longer and shorter structures are also observed due to particle breakage or end-to-end assembly – however overall the size distribution was narrow and the average length of TMV measured by TEM and using Image J analysis was 283 nm. The shorter length may be

explained due to breakage occurring during repeat ultracentrifugation during the purification or drying process during TEM grid preparation.

Next, PEGylated samples were imaged and overall TEM confirmed the structural integrity of the samples. High aspect ratio nanoparticles were observed for each formulation; TMV-PEG2K, TMV-PEG5KB, and TMV-PEG5K (Fig 4.8). The average size before and after PEG conjugation is shown in Table 4.1. I observed that the size homogeneity of the TMV nanoparticles varied after the conjugation process. This compares similarly to previous studies with PEGylation of TMV [48]. The shorter sizes of PEGylated vs the unmodified versions of TMGMV and TMV-Lys are explained by the additional processing, washing, and centrifugation steps upon chemical modification.

Table 4.1: Average length of PEGylated TMGMV and TMV

Particle Type	Average Particle Length (nm)
TMGMV	247± 52
TMGMV-PEG2K	138 ± 39
TMV-Lys	282 ± 13
TMV-PEG2K	216 ± 55
TMV-PEG5KB	210 ± 56
TMV-PEG5K	123 ± 31

Lastly, I analyzed the surface charge of all nanoparticle formulations by zeta potential (ζ) measurements (Table 4.2) – this will help understand the changes in soil mobility as a function of surface chemistry and hence the charge. The ζ of TMGMV is less negative compared to TMV-Lys which was earlier reported to be -8.0 ± 1.5 mV [43]. However, PEG molecules, which

are larger and also less negative, surround the surface of the VNP and result in the ζ being more neutral as previously reported [49]. This is the reason for the less negative ζ values observed after the PEGylation of these VNPs.

Table 4.2: Zeta potential (ζ) of native and PEGylated VNP

Sample Name	Zeta Potential Averages (ζ) (mV)
TMGMV	-6.43 ± 1.15
TMGMV-PEG2K	-1.89 ± 0.45
TMV-Lys	-25.28 ± 5.38
TMV-PEG2K	-12.22 ± 3.02
TMV-PEG5KB	–11.45 ± 0.37
TMV-PEG5K	-19.63 ± 2.57
PhMV	+4.20 ± 0.46 [50]
PVX	24.9 ± 8.2 [51]

Based on this characterization, I used native TMGMV, native TMV-Lys, TMGMV-PEG2K, TMV-PEG2K, TMV-PEG5KB, and TMV-PEG5K – all of which have a negative surface charge and PhMV and PVX – which carry positive surface charge – for the soil mobility assays. I did not proceed with TMGMV-PEG5K due to the formation of large aggregates and a low degree of conjugation.

4.2 Properties of soils

Table 4.4: Chemical composition (PPM) analysis by Western Laboratories for all the 4 different soil types used in this study

Soil Type	pH	Soluble Salts	NO_3	NH_4	P	K	Ca	Mg	S	Na	Zn	Cu	Mn	Fe	B
Magic Top Soil	6.0	0.3	1.0	6.0	10.0	70.0	128.0	18.0	91.0	23.0	4.1	1.0	11.2	5.5	0.3
Veggie	6.3	3.3	24.0	5.0	1.0	4.8	3.7	10.8	8.3	8.8	2.0	0.7	2.2	3.5	5.3
Potting	6.6	6.0	11.0	5.8	0.9	4.3	3.3	9.3	9.1	9.0	1.7	0.9	1.9	3.6	4.7
50/50	6.7	7.3	3.0	4.2	1.1	3.9	4.1	12.4	11.0	11.6	2.2	1.8	3.6	6.7	5.3

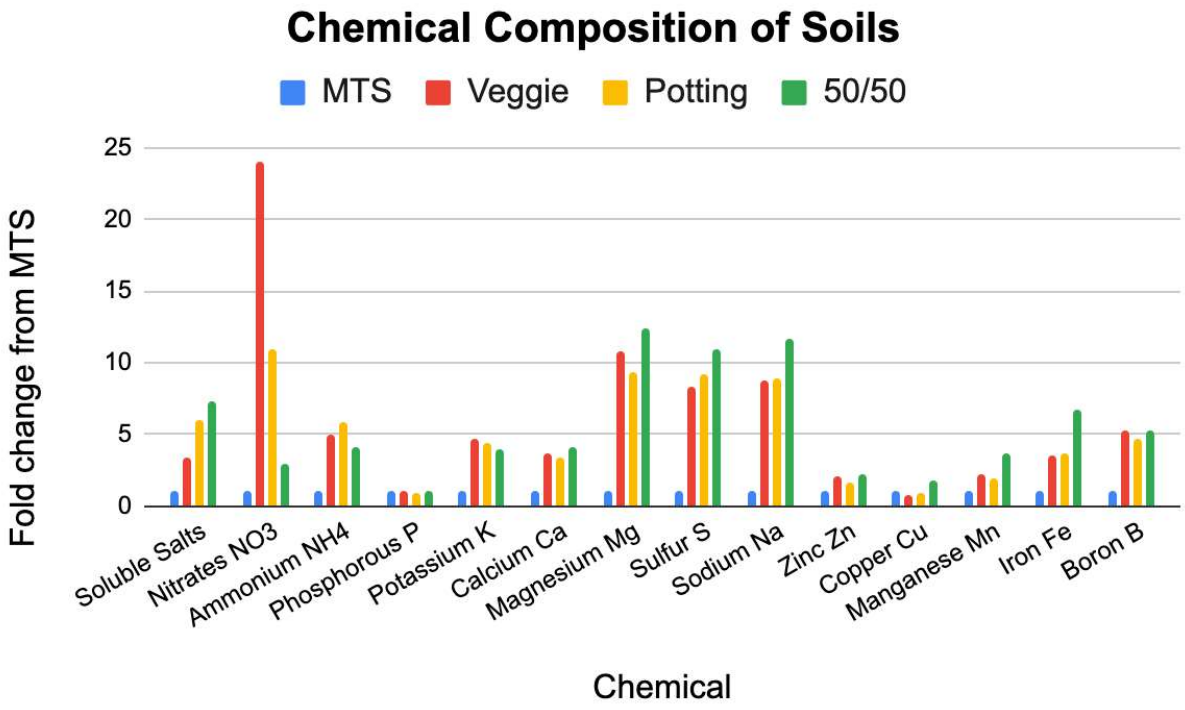

Figure 4.9: Illustration of the chemical composition of various soils tested vs MTS

There are noticeable differences in the chemical composition of the different soil types:

- The amount of Nitrates (NO_3) is very high in Veggie soil
- The amounts of Mg, S and Na is significantly higher Veggie, Potting, and 50/50 soil vs. MTS
- 50/50 seem to be the most nutrient-rich soil type based on high levels of Sodium, Sulfur, Magnesium and Iron present in the soil
- All the soil types are in general significantly more nutrient-rich than MTS

4.3 Brilliant Blue tracer assays for soil mobility and soil properties

To understand the elution behavior of our soil column system for small molecules, I first evaluated the elution of 1 mg of Brilliant Blue (2% v/v) from the soil columns; a flow rate of 5 mL min^{-1} was used. I hypothesized that the small molecules would flow out quickly with the water and not be hindered by the soil-particle interaction as much. Therefore, this assay will provide guidance for the design of the experiments with the VNPs, specifically providing guidance on which soil column height is feasible to test as a function of soil.

To conduct this experiment in the laboratory and to recreate the outdoor conditions such as rain and water flow from top to bottom, we set up the experiment similar to a previous soil mobility study that was conducted using VNP and synthetic nanoparticles [44]. Wet soil was packed into columns, the agent to be analyzed (Brilliant Blue or later the VNPs) then applied using a continued flow rate and a syringe pump.

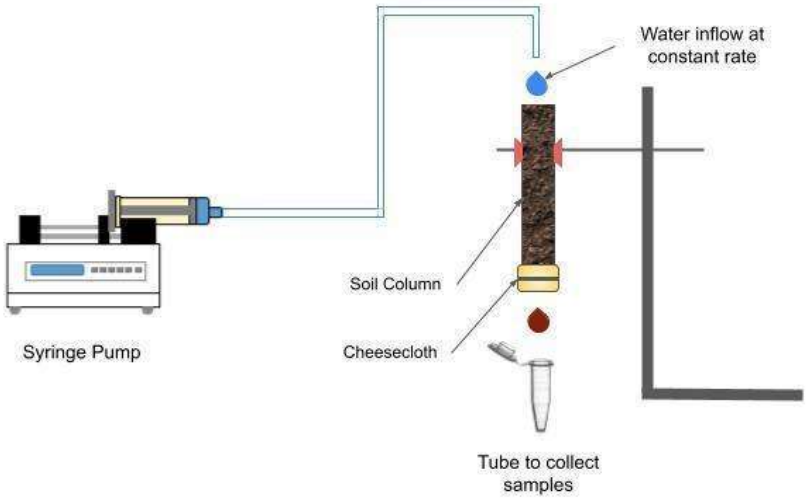

Figure 4.10: Experimental setup for soil mobility tests with constant flow rate

To measure the elution profile, several fractions were collected and analyzed using absorbance measurements at 590 nm (the maximum for Brilliant Blue). I measured the maximum soil packing density by filling the different soils into the soil columns to reach the maximum packing of soil and calculated the following parameters Void Fraction (φ), Void Volume (V_{void}) [Density of Soil = ρ, Max. Packing Density = ρ_{max}]:

Equation 1: $Void\ Fraction\ (\varphi) = \rho/\rho_{max}$

Equation 2: $Void\ Volume\ (V_{void}) = \varphi * V_{soil}$

Equation 3: $Relative\ Mobility\ (\mu) = (\varphi * V_{soil})/V_{max\ elution}$

This was done to understand the impact of air pockets that occur as a result of packing soil columns with prewetted soil. It should be noted, however, that this is an overapproximation of the Void Fraction (φ) because true max. packing density could not be achieved by hand, but this comparison is still a useful tool for making comparisons between the soil mobility at different depths

of soil. Table 3.4 shows the data we collected for Magic Top Soil (MTS), Veggie, Potting, and 50/50 soils.

Table 4.3: Calculated parameters describing the properties of the soil columns such as the Void Fraction (φ), Void Volume (V_{void}), and Relative Mobility (μ) for Magic Top Soil, Veggie, Potting, 50/50

Soil Type	Soil Volume (mL)	Density of Prewet Soil (g/mL)	Max. Packing Density (g/mL)	φ	Void Volume (V_{void})(mL)	Elution Volume (mL)*	Relative Mobility (μ)
MTS	10	0.67	0.9	0.74	7.44	4.00	1.86
	25	0.49	0.85	0.58	14.41	10.00	1.44
	50	0.42	0.86	0.49	24.42	16.00	1.53
	75	0.41	0.84	0.49	36.61	32.00	1.14
Veggie	15	0.62	1.19	0.52	7.82	8.00	0.98
Potting	15	0.61	1.36	0.45	6.73	6.00	1.12
50/50	5	1.06	0.84	1.26	6.30	12.00	0.52

*see Figure 4.11

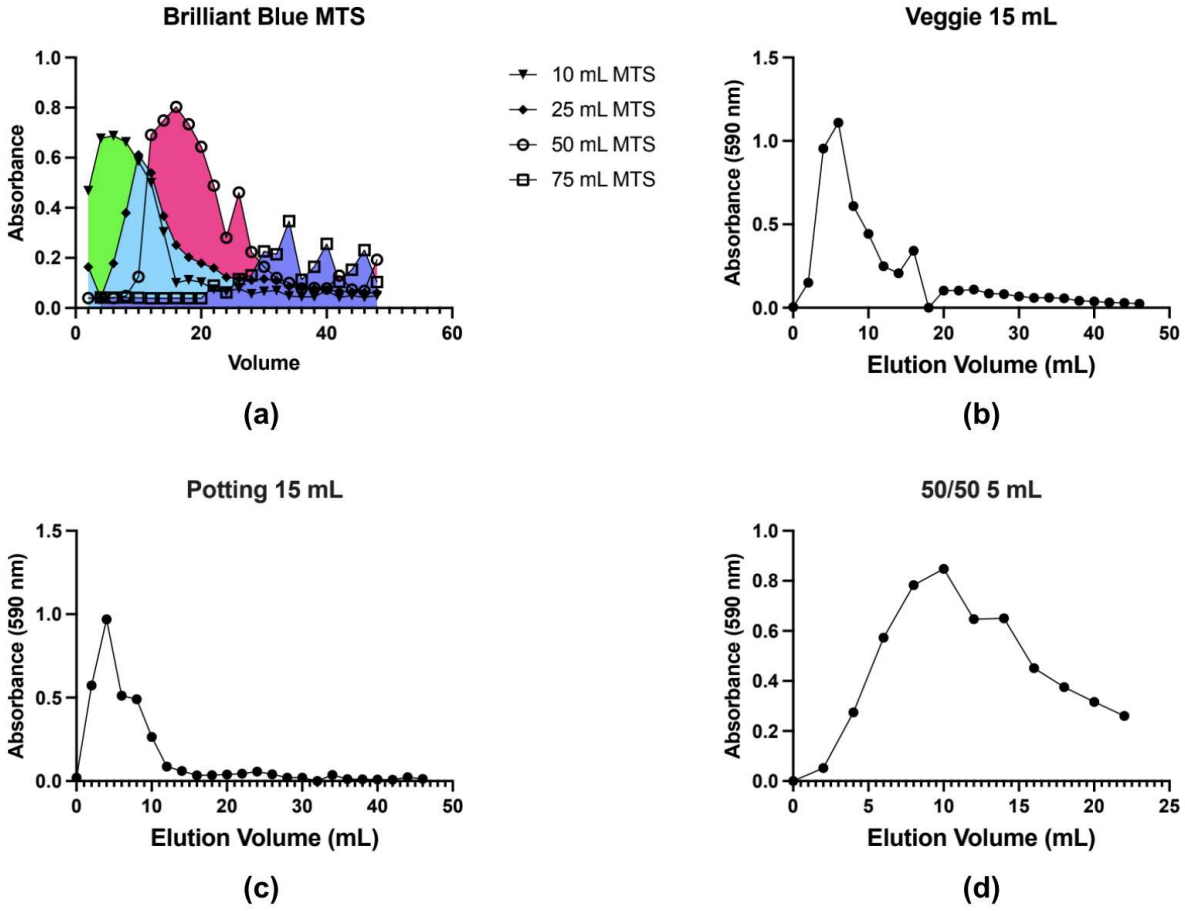

Figure 4.11 : Soil elution profile obtained for Brilliant Blue tracer molecules in soil columns using (a) MTS, (b) Veggie, (c) Potting, and (d) 50/50 soil types.

The small molecule (Brilliant Blue) has good mobility and elution peaks correlated with the void volume with a margin of consistent error. Figure 4.11 also provides clarity on the relationship between the mobility of Brilliant Blue and the soil type and its chemical compositions – hence packing density and void volume. There are also other physical differences between the soil types: the color, the texture, and the water retention capacity. Brilliant Blue molecules were expected to flow out with the waterfront, i.e. at the void volume. It is noted that the void volume likely is overestimated by the nature of the measurement – and this is reflected by the data: in MTS Brilliant blue consistently elutes at prior to the void volume and the effect is more apparent with increasing

columns length. In Veggie and Potting soil, Brilliant Blue elutes at the predicted void volume and at 50/50 past the void volume. This data, therefore, shows differences in soil mobility as a function of soil properties. Data suggest that small molecules have good mobility in MTS, lesser in Veggie/Potting, and more significantly reduced soil mobility in 50/50. This trend is also reflected in the calculated mobility (see Table 4.11)

4.4 Comparison between BCA and SDS-PAGE

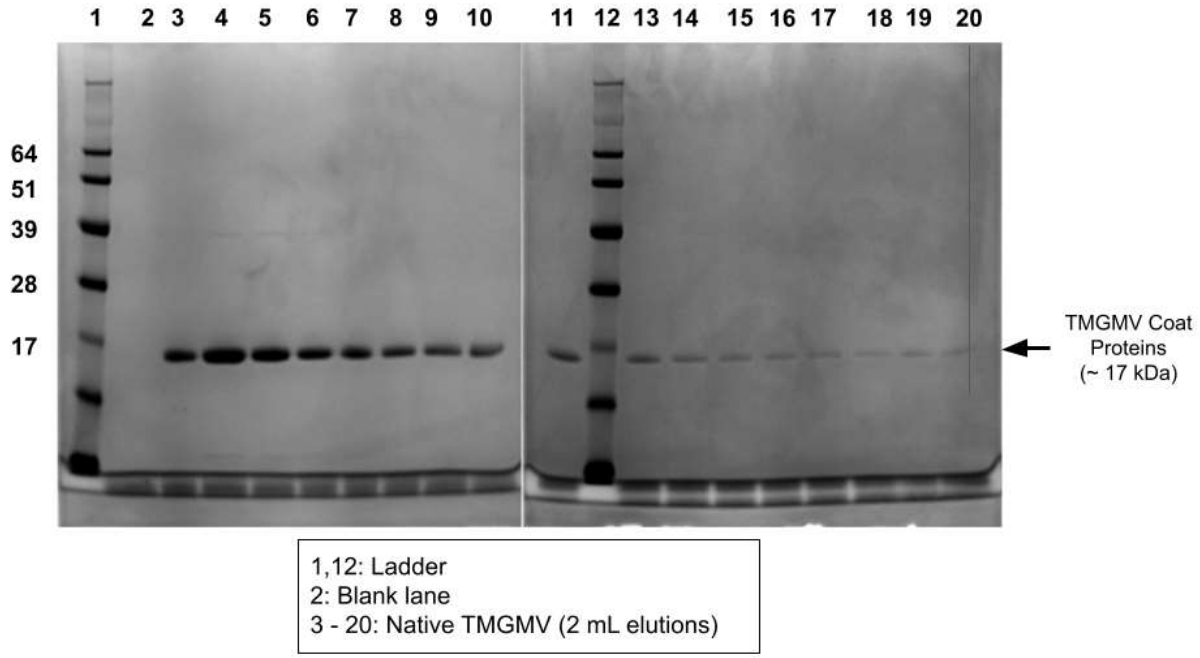

Figure 4.12: SDS-PAGE of native TMGMV in 10 mL MTS

Figure 4.12 shows the SDS-PAGE for samples collected using native TMGMV in 10 mL MTS, and we can observe the band intensity being the highest at 4 mL of elution of the sample. The band intensity gradually decreases as the elution volume increases. This high-intensity band shows the elution volume where the highest concentration of CP was flushed out.

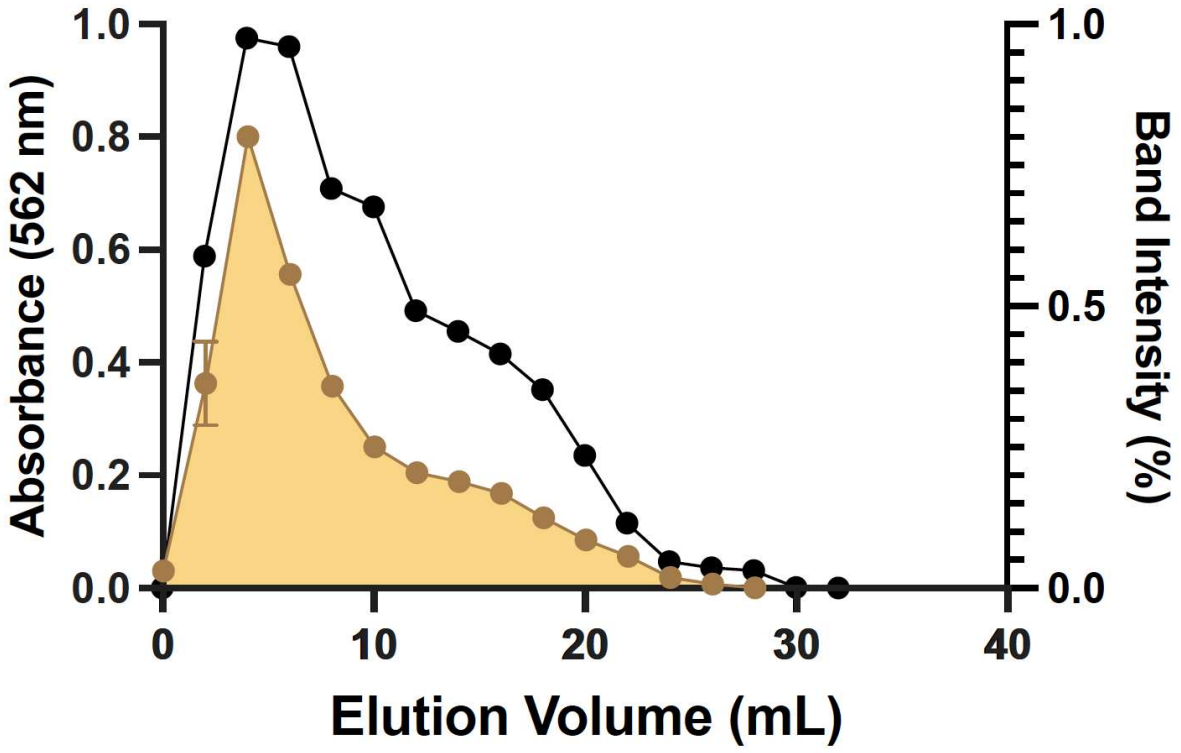

Figure 4.13: BCA elution profile with the area under the curve analysis (AUC) and band intensity analysis of SDS-PAGE for native TMGMV in 10 mL MTS

Figure 4.13 shows the BCA elution profile for native TMGMV in 10 mL MTS. The elution volume where a peak in absorbance is observed is at 4 mL. This corresponds to the high-intensity band in Figure 4.12. Using this comparison, we can suggest that the BCA was able to provide more accurate results are a higher throughput compared to SDS-PAGE. We were able to analyze the data from BCA much quicker than performing lane analysis to obtain information on the elution volume, and the amount of protein washed out based on the intensity. The AUC analysis (Figure 4.13), which was performed using the data from the BCA profile, reveals the amount of the protein that is washed out from the soil column with more accuracy. From this comparison, we can infer that for soil mobility studies, BCA protein assay is a more sensitive protein detection method when compared to SDS-PAGE.

4.5 MTS with VNP formulations

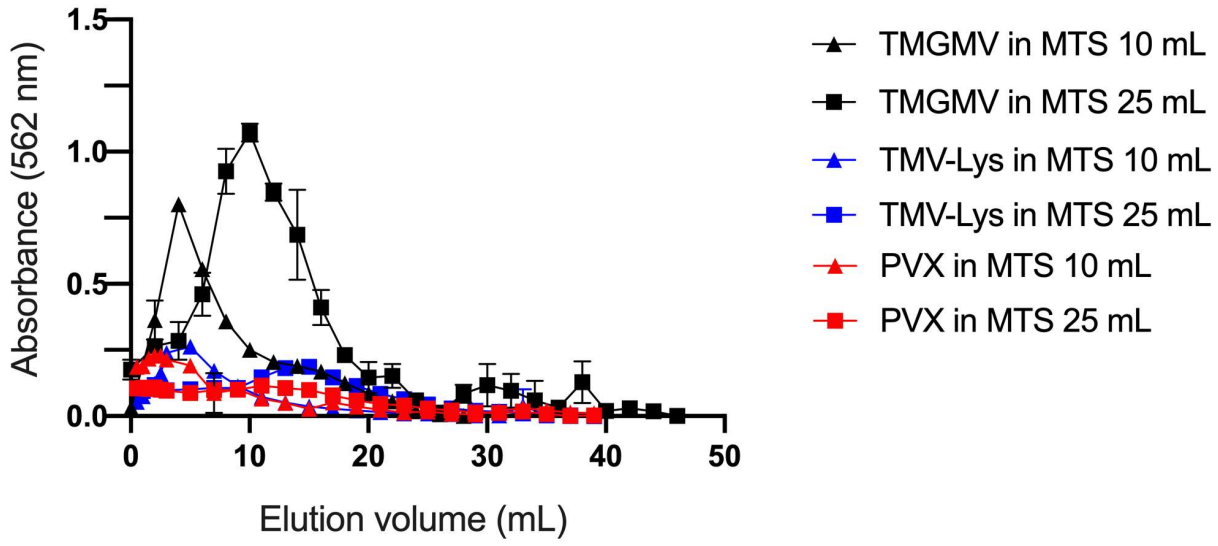

Figure 4.14 : Soil mobility of native TMGMV, native TMV, and native PVX VNPs in MTS

I analyzed and compared the soil mobility of TMV-Lys vs. TMGMV and PVX in MTS using 10 mL and 25 mL columns. TMGMV showed good soil mobility (Figure 4.14), which is consistent with prior reports [44]. Data in Figure 4.14 indicate that the soil mobility of TMV-Lys vs. TMGMV and PVX is distinct with only a small fraction of the proteins eluting. There is a possibility that the BCA assay requires more optimization and/or is not suitable for all nanoparticle platforms. Our data indicate that while TMGMV has good soil mobility, TMV-Lys does not elute from the column. This is somewhat puzzling but may indicate that soil behavior is strongly correlated to surface chemistry. Although both TMGMV and TMV-Lys have a similar structure, the key difference is the Lysine corona on TMV-Lys that may promote more interactions with soil. If not taking into account the amount of particle eluted but the elution peak, data also indicate that TMV-Lys elutes at later time points – again suggesting enhanced soil interactions (Figure 4.14). PVX, with a filamentous structure, also appears to not elute well from the soil column with very little protein detected in the BCA assay.

While often used in the laboratory setting, MTS is not the primary type of soil that's used in mass-production commercial agricultural practices. Therefore there is a need to understand how these VNPs perform in soil types that are commonly used for such agricultural purposes. We selected three different soil types: Potting, Veggie, and 50/50 mix for their diverse applications.

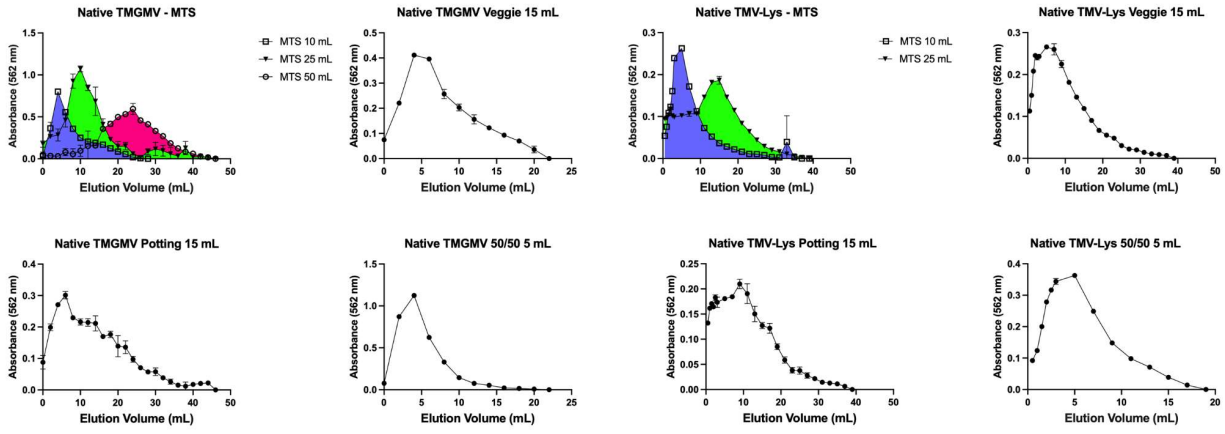

Figure 4.15: Elution profile of native TMGMV and TMV-Lys in all different soil types (MTS, Veggie, Potting, and 50/50)

The difference in the surface chemistry of the VNPs as well as the difference in the chemical composition of the soil result in producing unique elution profiles for the VNPs. Noticeable changes due to changes in the surface chemistry of the VNP can be observed in Figure 4.15, where native TMGMV was compared with TMV-Lys in different soils. The less negatively charged TMGMV washed out quicker compared to TMV-Lys with positive Lys corona. This may also substantiate that altering or modifying the surface of the VNP has a great impact on its behavior in the soil. For comparison: from a 25 mL soil column, TMGMV eluted at 10 mL and TMV-Lys at 15 mL, this again may indicate that the Lys corona promotes more soil-particle interactions. And this trend was consistent across the various soils that were analyzed (Figures 4.15 and 4.16).

4.6 Surface modified VNP formulations

An extended study was then performed on surface modified VNPs to shed more light on the impact of surface chemistry on the soil transport behavior of these particles. PEG, a biocompatible polymer chain with different molecular weights was used for modifying the surface of TMGMV and TMV-Lys (Figures 4.16 and Table 4.5)

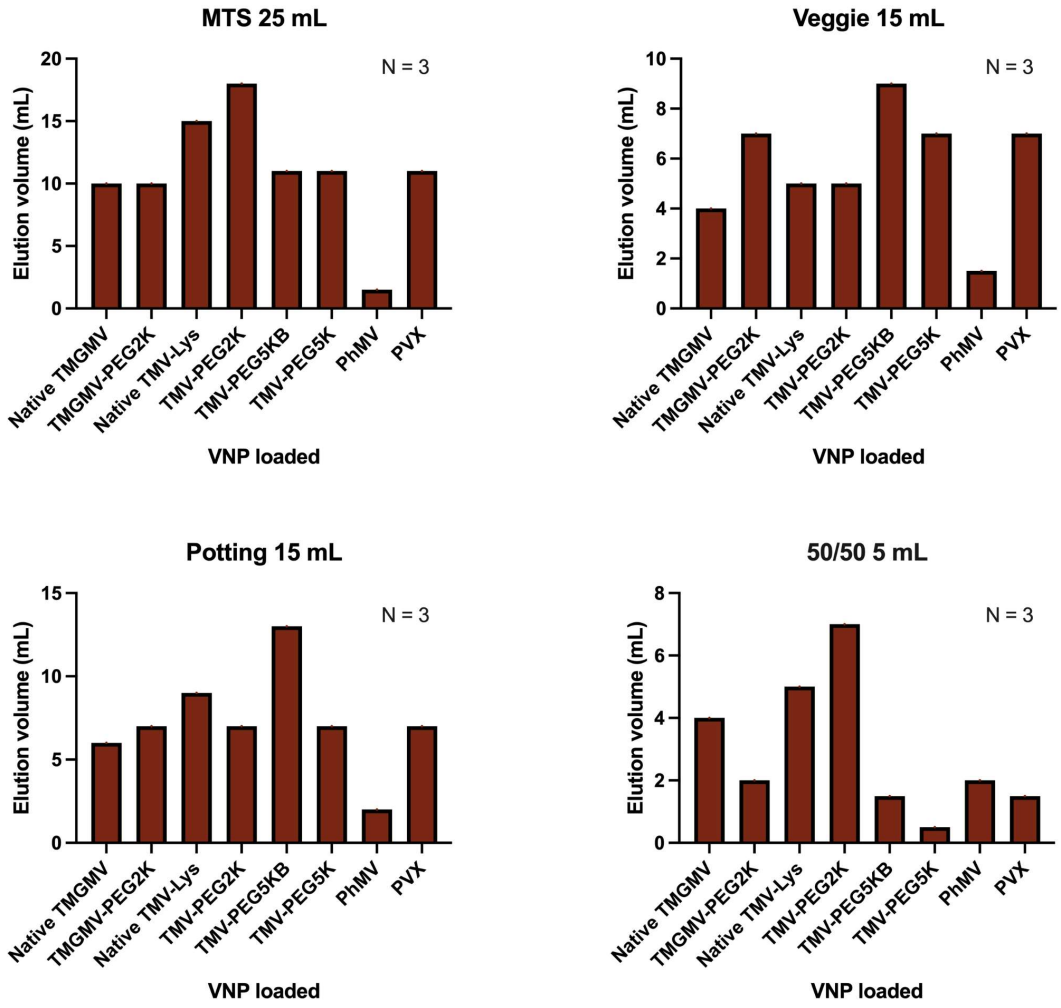

Figure 4.16 : Soil mobility profile for PEGylated TMGMV and TMV-Lys in different soil types

Table 4.5: Elution volume for VNPs in different soils

	MTS 10 mL	MTS 25 mL	MTS 50 mL	MTS 75 mL	Veggie 15 mL	Potting 15 mL	50/50 5 mL
TMGMV	4	10	24	-	4	6	4
TMGMV-PEG2K	4	10	10	24	7	7	2
TMV Lys	5	15	19	-	5	9	5
TMV-PEG2K	3	18	-	-	5	7	7
TMV-PEG5KB	5	11	-	-	9	13	1.5
TMV-PEG5K	7	11	-	-	7	7	0.5
PhMV	1.5	1.5	-	-	1.5	2	2
PVX	2	11	13	-	7	7	1.5

The data suggests that modifying the surface of the VNP provides greater control over the mobility of these particles. The impact on VNP-soil mobility can be inferred from Figure 4.16: selective VNPs with surface modification performed best in certain soils. For example, we can note that TMV-PEG2K performed as the top candidate in MTS as well as 50/50 soil whereas TMV-PEG5KB performed better in Veggie and Potting soils. However, the data also shows that there is no universal VNP modification that would work in all soils. More work is needed to understand these phenomena and future studies could include more types of soils and more VNP formulations to further understand the impact of their soil chemistry on the performance of these particles.

While differences are observed comparing the various formulations; differences are subtle and clear trends do not emerge (see also discussion below). The most striking feature is that data suggests that small icosahedrons perform best, i.e. PhMV had the highest soil mobility – and when comparing soil mobility of TMGMV, TMV-Lys, and PVX – the rod-shaped and filamentous nanoparticles all performed similarly. The lower mobility may be explained by the high aspect ratio nanoparticle shape that may lead to increased soil-particle interactions.

However, it should be noted that while TMGMV's mobility is lower in soil compared to PhMV – this may be an advantage and avoid leaching into groundwater.

Next, I calculated the mobility in soil using equation 3. The data is plotted and tabulated in Figure 4.17 and Table 4.6.

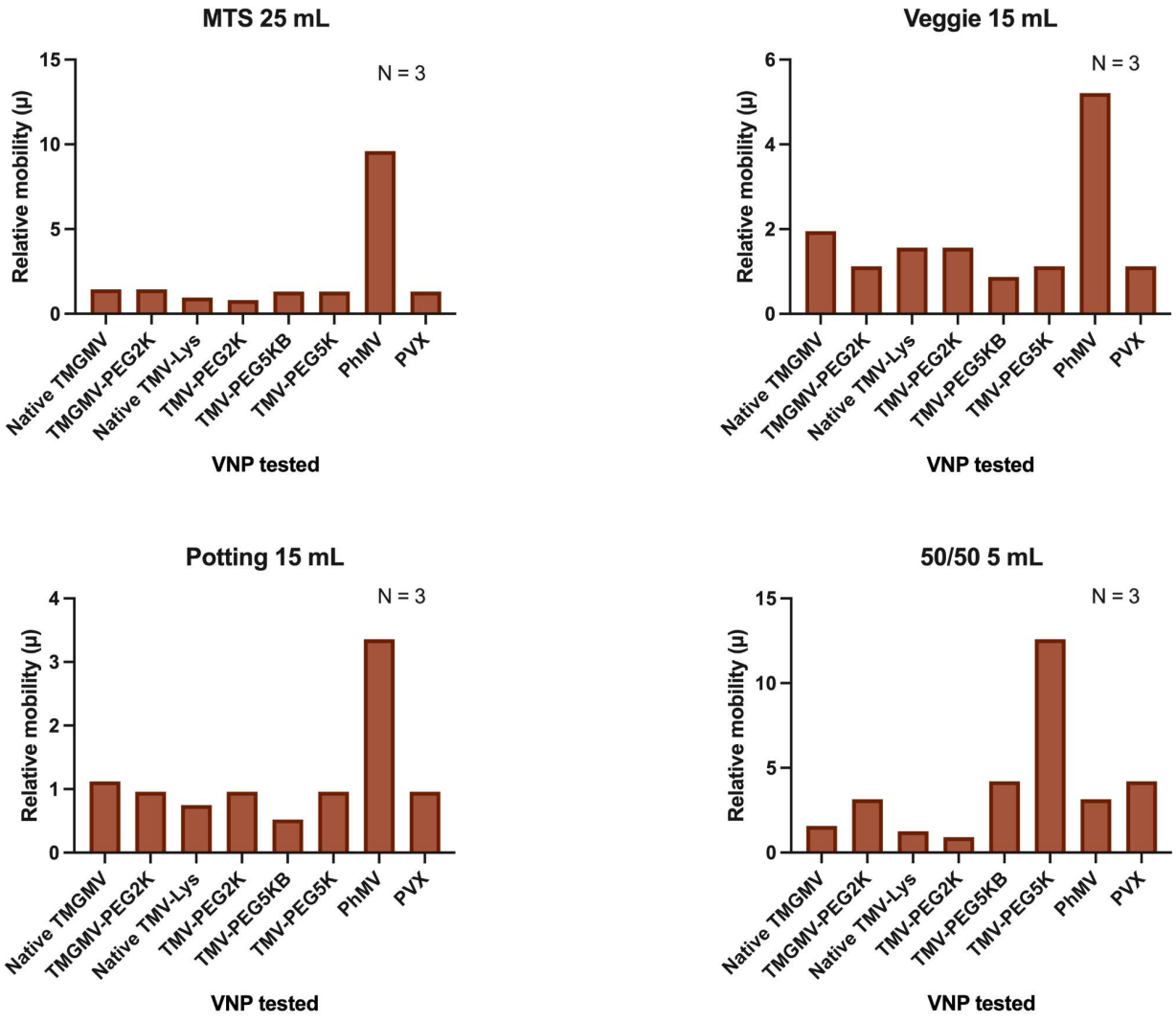

Figure 4.17: Relative mobility of native and surface modified VNPs

Table 4.6: Summary of relative mobility of VNP in different soil types

VNP \ Soil type and depth	MTS 10 mL	MTS 25 mL	MTS 50 mL	MTS 75 mL	Veggie 15 mL	Potting 15 mL	50/50 5 mL
TMGMV	1.86	1.44	1.02	-	1.95	1.12	1.57
TMGMV-PEG2K	1.86	1.44	2.44	1.53	1.12	0.96	3.15
TMV-Lys	1.49	0.96	1.29	-	1.56	0.75	1.26
TMV-PEG2K	2.48	0.80	-	-	1.56	0.96	0.90
TMV-PEG5KB	1.49	1.31	-	-	0.87	0.52	4.20
TMV-PEG5K	1.06	1.31	-	-	1.12	0.96	12.60
PhMV	4.96	9.61	-	-	5.21	3.36	3.15
PVX	3.72	1.31	1.88		1.12	0.96	4.20

This data shows the following trends:

(1) TMGMV has better soil mobility compared to TMV-Lys.

(2) The longer the columns, the lower the mobility – this trend is explained by the longer soil-particle interactions as well as dispersion type effects.

(3) For the PEGylated TMGMV there was no clear trend for the changes in mobility: same mobility in MTS 10 mL and 25 mL, higher mobility in 50 mL MTS, lower mobility in Veggie and Potting soil, yet faster mobility in 50/50 soil. This may indicate that there is no unified correlation between the surface chemistry of the particle and its soil properties, but rather it needs to be optimized for each soil type separately.

(4) There is no clear trend either when comparing TMV-PEG2K vs TMV and its relationship to TMGMV-PEG2K vs TMGMV.

(5) The most noticeable changes were observed with PhMV – which consistently had the highest mobility, likely because it is the smallest particle measuring only 30 nm. This data however contradicts previously published data [44]. Differences in soil and experimental setup may be the explanation.

Figure 4.17 elaborates on the soil mobility behavior showing the VNPs with the highest soil mobility, i.e. fastest to flush out without any significant interaction or affinity with the soil particles. PhMV has the highest relative mobility due to its shape and size compared to the rod-like and filamentous VNPs. This data also shows the importance of surface modification as well as the effect of surface modification on the soil mobility of these VNPs.

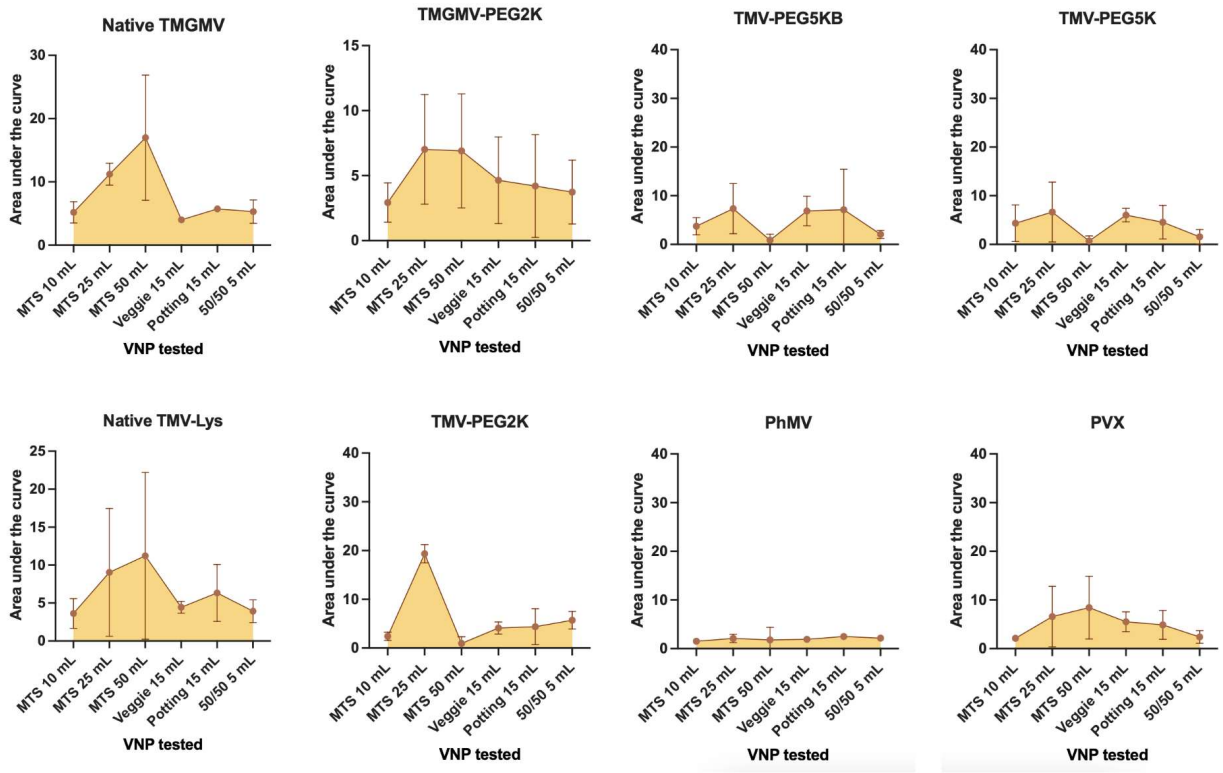

Figure 4.18: Area under the curve (AUC) analysis for VNPs in different soils

Table 4.7: Summary of AUC analysis for VNPs in different soils

	MTS 10 mL	MTS 25 mL	MTS 50 mL	Veggie 15 mL	Potting 15 mL	50/50 5 mL
TMGMV	6	12	10	4	5	7
TMGMV-PEG2K	1.85	4.03	3.8	2.29	1.41	5.48
TMV-Lys	2.25	3.09	3.45	3.9	3.68	2.88
TMV-PEG2K	2	21	2	3	2	4
TMV-PEG5KB	2.5	3.7	1.8	4.7	1.2	2.6
TMV-PEG5K	1.7	2.3	1.4	5	2.1	2.6
PhMV	1.6	2.7	3.6	2.4	3	2.3
PVX	2.3	2.2	3.9	4.1	2.8	3.3

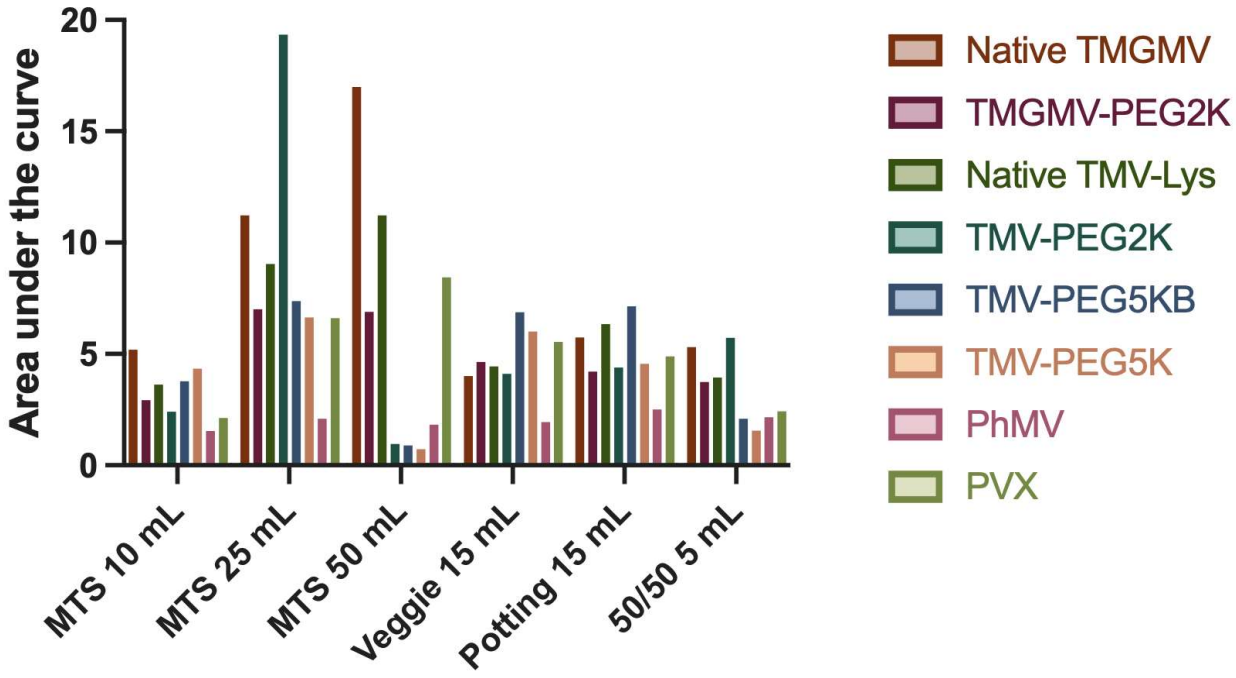

Figure 4.19: AUC analysis for VNPs in different soils

The area under the curve (AUC) analysis in Figure 4.18 represents the amount of protein recovered after the VNPs passed through the soil columns with different soil types. We can infer the absorptivity of the VNPs to the soil particles from this analysis. AUC analysis revealed that the amount of protein washed out of the columns were not uniform across all soils indicating

that CPs were bound to the soil surface more strongly in some soil types than the other for example Veggie soil which flushed out the least amount of native TMGMV and native TMV-Lys. However, for PhMV, we could observe almost a straight line graph indicating uniform recovery of CPs in all the different soil types. Surface modification seems to have impacted as increasing the soil volume decreased the amount of protein recovered, for example, 50 mL of MTS consistently had the lowest amount of protein recovered especially after PEGylation of the rod-like VNPs.

Chapter 5: Conclusions

In this study, we assessed the soil mobility behavior of rod-shaped VNPs derived from TMGMV and TMV-Lys. Specifically, we modified their surfaces with PEG and assessed changes in their retention behavior while running through irrigated soils at a constant flow rate. In doing so, we were able to investigate the effects of surface modification and particle size on the mobility of VNPs in soil. We investigated using 4 kinds of soil, each with different chemical and physical properties, which gave insights into some of the interactions between the soil and the soil mobility behavior of the VNPs. These initial data provide a framework for continuing these studies with variables such as protein concentration, PEG surface coverage, and other types of soils and surface modifications in the future.

Additionally, we learned that this mobility assay has some limitations. For more hydrophobic soils, a constant irrigation rate can be challenging for assessing mobility, as a pool of the liquid at the soil interface can skew the results. Further, large soil volumes can significantly dilute the sample, which can lead to errors due to the limit of detection of the experiment. Finding more chemically diverse soils to test in future studies may be fruitful, as they may accentuate differences in particle mobility by changing particle-soil interactions.

We showed that BCA is a powerful tool to make protein measurements from soil mobility more medium throughput than previous SDS-PAGE standards for VNPs. The use of BCA versus SDS-PAGE can lead to both time and cost savings by not having to prepare and stain multiple gels, and instead translating the experimental measurements to a 96-well plate. Particularly as protein-derived nanomaterials become more prevalent in agricultural applications, this new assay modification has the potential to benefit many researchers down the road.

This study is a start in expanding the knowledge base for VNP mobility behavior in the soil. By developing a new BCA-based approach to measuring the soil mobility, we have significantly improved the throughput of these measurements and made the data-driven experimental design more feasible. We also have demonstrated that surface modifications, soil depth, and particle type all do have varying degrees of contribution to soil mobility, but that surface modification seems to be the most influential in this study.

Chapter 6: Perspectives and Future Outlooks

The application of proteins and VNPs in agriculture remains a new field and when I started this research there were only 2 publications on VNP soil properties [52, 27]. However this data was limited and only one soil type was evaluated. Therefore there is a need to increase the knowledge on how plant VNPs behave in soil. This persuaded us to create a bank of knowledge on the soil behavior, surface modification, and all other important parameters that would allow us to use these pesticide nanocarriers on different soils to combat nematodes depending on the soil as well as the soil mobility characteristics of the VNPs. Specifically, I set out to conduct studies and perform research to dissect how soil type and nanoparticle surface chemistry impact the soil mobility of VNPs. By exploring the soil mobility characteristics of different VNPs, our research has contributed to a general understanding of the performance of these high-aspect-ratio pesticide carriers in the soil as well as the effect of surface modification on their soil mobility.

Due to the limitation of experimentation, we could only understand the soil behavior of two of the native VNP as well as their surface-modified counterparts. We were also limited to the use of only 4 different soil types – however, in agricultural practice, many more soil types are in use. With the help of Machine Learning (ML) and Artificial Intelligence (AI), there is great scope to develop predictive computational models for more efficient soil mobility studies. Using ML and AI, it would also be reliable to see predictive results on countermeasures being suggested for nematodes and crop infestations. Building a library of all known VNPs as well as their soil mobility characteristics would provide the foundation for such systems in the future.

Surface modification performed in this study was limited to PEG chains, but future studies could focus on using different biocompatible polymer alternatives to achieve improved

performance of these VNPs such as using Poly(N-(2-hydroxypropyl)methacrylamide which is a promising alternative to PEG by allowing for the formation of more complex shapes during conjugation [53] and also because of its ability decrease protein adsorption [54] which could translate to lower VNP aggregation and also soil-VNP interactions. Improved conjugation efficiency is another aspect that must be considered while researching surface-modified VNPs.

Another aspect of this work was to establish the BCA assay as a useful tool for mobility studies because of its medium throughput and lower incubation time as compared to running SDS-PAGE for a high volume of samples. However there is also room for improvement: There is also a great scope in the development of better methods for the detection of protein concentration, for example by combining different protein detection methods [55] we could get more sensitive results. We could also try to use different irrigation methods as well as irrigation rates to understand and recreate the natural rainfall conditions as well as indoor-garden-irrigation systems.

Literature data and data presented in this thesis suggest that high aspect ratio TMGMV makes a useful carrier for pesticides for soil applications. My data support the further development of this promising technology and highlight the need for systematic structure-function studies.

References

(1) World Food Programme. A global food crisis | World Food Programme https://www.wfp.org/global-hunger-crisis.

(2) Trellu, C.; Olvera Vargas, H.; Mousset, E.; Oturan, N.; Oturan, M. A. Electrochemical Technologies for the Treatment of Pesticides. Current Opinion in Electrochemistry 2021, 26.

(3) Lichtfouse, E.; Navarrete, M.; Debaeke, P.; Souchère, V.; Alberola, C.; Ménassieu, J. Agronomy for Sustainable Agriculture. A Review. Agronomy for Sustainable Development 2009, 29, 1–6.

(4) Jat, R. A.; Wani, S. P.; Sahrawat, K. L. Conservation Agriculture in the Semi-Arid Tropics. Advances in Agronomy 2012, 117, 191–273..

(5) Marino, M.; Mele, E.; Viggiano, A.; Nori, S. L.; Meccariello, R.; Santoro, A. Pleiotropic Outcomes of Glyphosate Exposure: From Organ Damage to Effects on Inflammation, Cancer, Reproduction and Development. Int. J. Mol. Sci. 2021, 22 (22), 12606. https://doi.org/10.3390/ijms222212606

(6) McCauley, L. A.; Anger, W. K.; Keifer, M.; Langley, R.; Robson, M. G.; Rohlman, D. Studying Health Outcomes in Farmworker Populations Exposed to Pesticides. *Environ. Health Perspect.* 2006, *114* (6), 953–960. https://doi.org/10.1289/ehp.8526.

(7) Shoiful, A.; Fujita, H.; Watanabe, I.; Honda, K. Concentrations of Organochlorine Pesticides (OCPs) Residues in Foodstuffs Collected from Traditional Markets in Indonesia. *Chemosphere* 2013, *90* (5), 1742–1750. https://doi.org/10.1016/j.chemosphere.2012.10.022.

(8) Tsakiris, I. N.; Goumenou, M.; Tzatzarakis, M. N.; Alegakis, A. K.; Tsitsimpikou, C.; Ozcagli, E.; Vynias, D.; Tsatsakis, A. M. Risk Assessment for Children Exposed to DDT Residues in Various Milk Types from the Greek Market. *Food Chem. Toxicol.* 2015, *75*, 156–165. https://doi.org/10.1016/j.fct.2014.11.012.

(9) Jones, R. A. C.; Naidu, R. A. Global Dimensions of Plant Virus Diseases: Current Status and Future Perspectives. *Annu. Rev. Virol.* 2019, *6* (1), 387–409. https://doi.org/10.1146/annurev-virology-092818-015606.

(10) Prasad, A.; Sharma, N.; Hari-Gowthem, G.; Muthamilarasan, M.; Prasad, M. Tomato Yellow Leaf Curl Virus: Impact, Challenges, and Management. *Trends Plant Sci.* 2020, *25* (9), 897–911. https://doi.org/10.1016/j.tplants.2020.03.015.

(11) Kalia, A.; Gosal, S. K. Effect of Pesticide Application on Soil Microorganisms. *Arch. Acker Pflanzenbau Bodenkd.* 2011, *57* (6), 569–596. https://doi.org/10.1080/03650341003787582.

(12) Sharma, A.; Kumar, V.; Shahzad, B.; Tanveer, M.; Sidhu, G. P. S.; Handa, N.; Kohli, S. K.; Yadav, P.; Bali, A. S.; Parihar, R. D.; Dar, O. I.; Singh, K.; Jasrotia, S.; Bakshi, P.; Ramakrishnan, M.; Kumar, S.; Bhardwaj, R.; Thukral, A. K. Worldwide Pesticide Usage and Its Impacts on Ecosystem. *SN Appl. Sci.* 2019, *1* (11). https://doi.org/10.1007/s42452-019-1485-1.

(13) Hub, I. S. K. *UNEP report identifies top actions to minimize adverse impacts of pesticides, fertilizers*. Iisd.org. https://sdg.iisd.org/news/unep-report-identifies-top-actions-to-minimize-adverse-impacts-of-pesticides-fertilizers/ (accessed 2022-11-08).

(14) Potrykus, I. Golden Rice and Beyond. *Plant Physiol.* 2001, *125* (3), 1157–1161. https://doi.org/10.1104/pp.125.3.1157.

(15) Dodson, L. *Recent trends in GE adoption*. Usda.gov. https://www.ers.usda.gov/data-products/adoption-of-genetically-engineered-crops-in-the-u-s/recent-trends-in-ge-adoption/ (accessed 2022-11-08).

(16) Hazarika, A.; Yadav, M.; Yadav, D. K.; Yadav, H. S. An Overview of the Role of Nanoparticles in Sustainable Agriculture. *Biocatal. Agric. Biotechnol.* 2022, *43* (102399), 102399. https://doi.org/10.1016/j.bcab.2022.102399.

(17) Li, L.; Xu, Z.; Kah, M.; Lin, D.; Filser, J. Nanopesticides: A Comprehensive Assessment of Environmental Risk Is Needed before Widespread Agricultural Application. *Environ. Sci. Technol.* 2019, *53* (14), 7923–7924. https://doi.org/10.1021/acs.est.9b03146.

(18) Huang, B.; Chen, F.; Shen, Y.; Qian, K.; Wang, Y.; Sun, C.; Zhao, X.; Cui, B.; Gao, F.; Zeng, Z.; Cui, H. Advances in Targeted Pesticides with Environmentally Responsive Controlled Release by Nanotechnology. *Nanomaterials (Basel)* 2018, *8* (2). https://doi.org/10.3390/nano8020102.

(19) De, A.; Bose, R.; Kumar, A.; Mozumdar, S. *Targeted Delivery of Pesticides Using Biodegradable Polymeric Nanoparticles*; Springer India: New Delhi, 2014.

(20) Chariou, P. L.; Ortega-Rivera, O. A.; Steinmetz, N. F. Nanocarriers for the Delivery of Medical, Veterinary, and Agricultural Active Ingredients. *ACS Nano* 2020, *14* (3), 2678–2701. https://doi.org/10.1021/acsnano.0c00173.

(21) Syafrudin, M.; Kristanti, R. A.; Yuniarto, A.; Hadibarata, T.; Rhee, J.; Al-Onazi, W. A.; Algarni, T. S.; Almarri, A. H.; Al-Mohaimeed, A. M. Pesticides in Drinking Water-A Review. *Int. J. Environ. Res. Public Health* 2021, *18* (2), 468. https://doi.org/10.3390/ijerph18020468.

(22) Shi, J.; Wu, Y.; Zhang, S.; Tian, Y.; Yang, D.; Jiang, Z. Bioinspired Construction of Multi-Enzyme Catalytic Systems. *Chem. Soc. Rev.* 2018, *47* (12), 4295–4313. https://doi.org/10.1039/c7cs00914c.

(23) Balique, F.; Lecoq, H.; Raoult, D.; Colson, P. Can Plant Viruses Cross the Kingdom Border and Be Pathogenic to Humans? *Viruses* 2015, *7* (4), 2074–2098. https://doi.org/10.3390/v7042074.

(24) Current ICTV taxonomy release. Ictv.global. https://ictv.global/taxonomy (accessed 2022-11-09).

(25) Kushnir, N.; Streatfield, S. J.; Yusibov, V. Virus-like Particles as a Highly Efficient Vaccine Platform: Diversity of Targets and Production Systems and Advances in Clinical Development. Vaccine 2012, 31 (1), 58–83. https://doi.org/10.1016/j.vaccine.2012.10.083.

(26) Chariou, P. L.; Ma, Y.; Hensley, M.; Rosskopf, E. N.; Hong, J. C.; Charudattan, R.; Steinmetz, N. F. Inactivated Plant Viruses as an Agrochemical Delivery Platform. ACS Agric. Sci. Technol. 2021, 1 (3), 124–130. https://doi.org/10.1021/acsagscitech.1c00083.

(27) Chariou, P. L.; Steinmetz, N. F. Delivery of Pesticides to Plant Parasitic Nematodes Using Tobacco Mild Green Mosaic Virus as a Nanocarrier. ACS Nano 2017, 11 (5), 4719–4730. https://doi.org/10.1021/acsnano.7b00823.

(28) Zaitlin, M. Elucidation of the Genome Organization of Tobacco Mosaic Virus. Philos. Trans. R. Soc. Lond. B Biol. Sci. 1999, 354 (1383), 587–591. https://doi.org/10.1098/rstb.1999.0410.

(29) Dawson, W. O.; Hilf, M. E. Host-Range Determinants of Plant Viruses. Annu. Rev. Plant Physiol. Plant Mol. Biol. 1992, 43 (1), 527–555. https://doi.org/10.1146/annurev.pp.43.060192.002523.

(30) Lin, R. D., Department of Biomedical Engineering, Case Western Reserve University, Cleveland, OH 44106, USA; Steinmetz, N. F. Tobacco Mosaic Virus Delivery of Mitoxantrone for Cancer Therapy. Nanoscale 2018, 10 (34), 16307–16313. https://doi.org/10.1039/c8nr04142c.

(31) Yi, H.; Rubloff, G. W.; Culver, J. N. TMV Microarrays: Hybridization-Based Assembly of DNA-Programmed Viral Nanotemplates. Langmuir 2007, 23 (5), 2663–2667. https://doi.org/10.1021/la062493c.

(32) Yildiz, I.; Lee, K. L.; Chen, K.; Shukla, S.; Steinmetz, N. F. Infusion of Imaging and Therapeutic Molecules into the Plant Virus-Based Carrier Cowpea Mosaic Virus: Cargo-Loading and Delivery. *J. Control. Release* 2013, *172* (2), 568–578. https://doi.org/10.1016/j.jconrel.2013.04.023.

(33) Lam, P.; Steinmetz, N. F. Delivery of SiRNA Therapeutics Using Cowpea Chlorotic Mottle Virus-like Particles. *Biomater. Sci.* 2019, *7* (8), 3138–3142. https://doi.org/10.1039/c9bm00785g.

(34) Le, D. H. T.; Lee, K. L.; Shukla, S.; Commandeur, U.; Steinmetz, N. F. Potato Virus X, a Filamentous Plant Viral Nanoparticle for Doxorubicin Delivery in Cancer Therapy. Nanoscale 2017, 9 (6), 2348–2357. https://doi.org/10.1039/c6nr09099k.

(35) Wege, C.; Koch, C. From Stars to Stripes: RNA-Directed Shaping of Plant Viral Protein Templates-Structural Synthetic Virology for Smart Biohybrid Nanostructures. *Wiley Interdiscip. Rev. Nanomed. Nanobiotechnol.* 2020, *12* (2), e1591. https://doi.org/10.1002/wnan.1591.

(36) Atabekov, J.; Nikitin, N.; Arkhipenko, M.; Chirkov, S.; Karpova, O. Thermal Transition of Native Tobacco Mosaic Virus and RNA-Free Viral Proteins into Spherical Nanoparticles. *J. Gen. Virol.* 2011, *92* (Pt 2), 453–456. https://doi.org/10.1099/vir.0.024356-0.

(37) Nikitin, N.; Ksenofontov, A.; Trifonova, E.; Arkhipenko, M.; Petrova, E.; Kondakova, O.; Kirpichnikov, M.; Atabekov, J.; Dobrov, E.; Karpova, O. Thermal Conversion of Filamentous Potato Virus X into Spherical Particles with Different Properties from Virions. *FEBS Lett.* 2016, *590* (10), 1543–1551. https://doi.org/10.1002/1873-3468.12184.

(38) González-Gamboa, I.; Caparco, A. A.; McCaskill, J. M.; Steinmetz, N. F. Bioconjugation Strategies for Tobacco Mild Green Mosaic Virus. *Chembiochem* 2022, *23* (18), e202200323. https://doi.org/10.1002/cbic.202200323.

(39) Dawson, W. O.; Lehto, K. M. Regulation of Tobamovirus Gene Expression. *Adv. Virus Res.* 1990, *38*, 307–342. https://doi.org/10.1016/s0065-3527(08)60865-9.

(40) Caciagli, P. Vegetable Viruses. In *Encyclopedia of Virology*; Elsevier, 2008; pp 282–290.

(41) Borovsky, D.; Rabindran, S.; Dawson, W. O.; Powell, C. A.; Iannotti, D. A.; Morris, T. J.; Shabanowitz, J.; Hunt, D. F.; DeBondt, H. L.; DeLoof, A. Expression of Aedes Trypsin-Modulating Oostatic Factor on the Virion of TMV: A Potential Larvicide. Proc. Natl. Acad. Sci. U. S. A. 2006, 103 (50), 18963–18968. https://doi.org/10.1073/pnas.0606146103.

(42) Environmental Protection Agency. Tobacco Mild Green Mosaic Tobamovirus (TMGMV); Temporary Exemption from the Requirement of a Tolerance. *Federal Register*. June 27, 2007, pp 35178–35181.

(43) Tiu, B. D. B.; Kernan, D. L.; Tiu, S. B.; Wen, A. M.; Zheng, Y.; Pokorski, J. K.; Advincula, R. C.; Steinmetz, N. F. Electrostatic Layer-by-Layer Construction of Fibrous TMV Biofilms. *Nanoscale* 2017, *9* (4), 1580–1590. https://doi.org/10.1039/c6nr06266k.

(44) Chariou, P. L.; Dogan, A. B.; Welsh, A. G.; Saidel, G. M.; Baskaran, H.; Steinmetz, N. F. Soil Mobility of Synthetic and Virus-Based Model Nanopesticides. *Nat. Nanotechnol.* 2019, *14* (7), 712–718. https://doi.org/10.1038/s41565-019-0453-7.

(45) Alonso Villela, S. M.; Kraïem, H.; Bouhaouala-Zahar, B.; Bideaux, C.; Aceves Lara, C. A.; Fillaudeau, L. A Protocol for Recombinant Protein Quantification by Densitometry. *Microbiologyopen* 2020, *9* (6), 1175–1182. https://doi.org/10.1002/mbo3.1027.

(46) Evtushenko, E. A.; Ryabchevskaya, E. M.; Nikitin, N. A.; Atabekov, J. G.; Karpova, O. V. Plant Virus Particles with Various Shapes as Potential Adjuvants. *Sci. Rep.* 2020, *10* (1), 10365. https://doi.org/10.1038/s41598-020-67023-4.

(47) Liu, T.; Thierry, B. A Solution to the PEG Dilemma: Efficient Bioconjugation of Large Gold Nanoparticles for Biodiagnostic Applications Using Mixed Layers. *Langmuir* 2012, *28* (44), 15634–15642. https://doi.org/10.1021/la301390u.

(48) Bruckman, M. A.; Randolph, L. N.; VanMeter, A.; Hern, S.; Shoffstall, A. J.; Taurog, R. E.; Steinmetz, N. F. Biodistribution, Pharmacokinetics, and Blood Compatibility of Native and PEGylated Tobacco Mosaic Virus Nano-Rods and -Spheres in Mice. Virology 2014, 449, 163–173. https://doi.org/10.1016/j.virol.2013.10.035.

(49) Shi, L.; Zhang, J.; Zhao, M.; Tang, S.; Cheng, X.; Zhang, W.; Li, W.; Liu, X.; Peng, H.; Wang, Q. Effects of Polyethylene Glycol on the Surface of Nanoparticles for Targeted Drug Delivery. Nanoscale 2021, 13 (24), 10748–10764. https://doi.org/10.1039/d1nr02065j.

(50) Masarapu, H.; Patel, B. K.; Chariou, P. L.; Hu, H.; Gulati, N. M.; Carpenter, B. L.; Ghiladi, R. A.; Shukla, S.; Steinmetz, N. F. Physalis Mottle Virus-like Particles as Nanocarriers for Imaging Reagents and Drugs. Biomacromolecules 2017, 18 (12), 4141–4153. https://doi.org/10.1021/acs.biomac.7b01196.

(51) Shukla, S.; Ablack, A. L.; Wen, A. M.; Lee, K. L.; Lewis, J. D.; Steinmetz, N. F. Increased Tumor Homing and Tissue Penetration of the Filamentous Plant Viral Nanoparticle Potato Virus X. Mol. Pharm. 2013, 10 (1), 33–42. https://doi.org/10.1021/mp300240m.

(52) Cao, J.; Guenther, R. H.; Sit, T. L.; Lommel, S. A.; Opperman, C. H.; Willoughby, J. A. Development of Abamectin Loaded Plant Virus Nanoparticles for Efficacious Plant Parasitic Nematode Control. ACS Appl. Mater. Interfaces 2015, 7 (18), 9546–9553. https://doi.org/10.1021/acsami.5b00940.

(53) Wright, T. A.; Page, R. C.; Konkolewicz, D. Polymer Conjugation of Proteins as a Synthetic Post-Translational Modification to Impact Their Stability and Activity. Polym. Chem. 2019, 10 (4), 434–454. https://doi.org/10.1039/C8PY01399C.

(54) Hadjesfandiari, N.; Parambath, A. Stealth Coatings for Nanoparticles. In Engineering of Biomaterials for Drug Delivery Systems; Elsevier, 2018; pp 345–361.

(55) Olson, B. J. S. C.; Markwell, J. Assays for Determination of Protein Concentration. Curr. Protoc. Pharmacol. 2007, Appendix 3 (1), 3A. https://doi.org/10.1002/0471141755.pha03as38.